Blowoff Dynamics and its Measurements

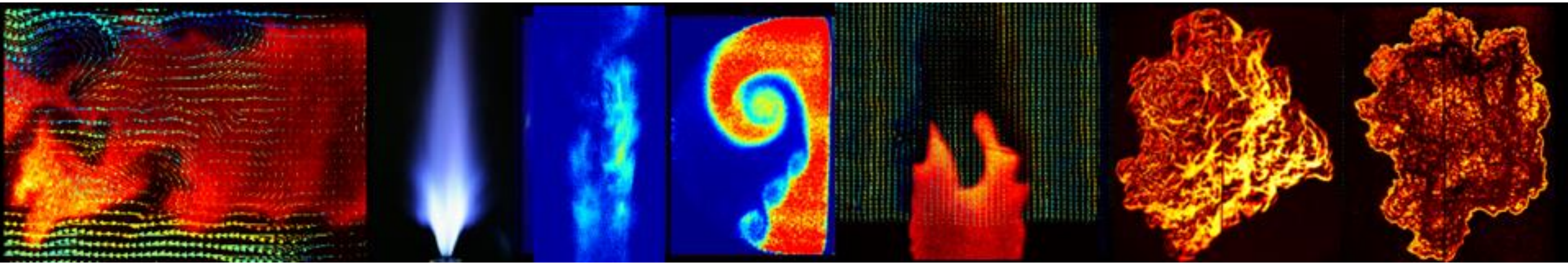

TANGO Workshop 5-7 February, IIT Madras

Swetaprovo Chaudhuri
Assistant Professor
Department of Aerospace Engineering
Indian Institute of Science

Bluff body and swirl stabilized flames

Bluff body and swirl stabilized flames are ubiquitous in propulsion and land based power generation systems

Aerospace propulsion: Ramjet and turbojet afterburners and even scramjets, industrial combustion systems, boilers and heat recovery steam generators use bluff body flame stabilizations.

Most gas turbine combustors: swirl flames.

Basic motivation behind use of a bluff body or swirl: To create a local low velocity recirculating flow region that continuously ignites the fresh mixture and sustains reactions in an otherwise high speed flow.

Blowoff

- Only within a certain range of conditions governed by fluid mechanics and chemical kinetics a flame can be stabilized by a bluff body.

- Even though it is trivial enough to assume correctly that leaning out the fuel concentration will lead to flame extinction and blowoff , its exact mechanism remained unsolved with works presented in *over 150 articles over the last five decades.*

Flame blowoff in the SR-71 during a high-acceleration turn, Campbell and Chambers

Campbell and Chambers, Patterns in the sky
S. Shanbhogue, S. Husain, T. Lieuwen, Progress in Energy and Combustion Science, 2009

Characteristics of flows separated by bluff bodies: Non-reacting flows

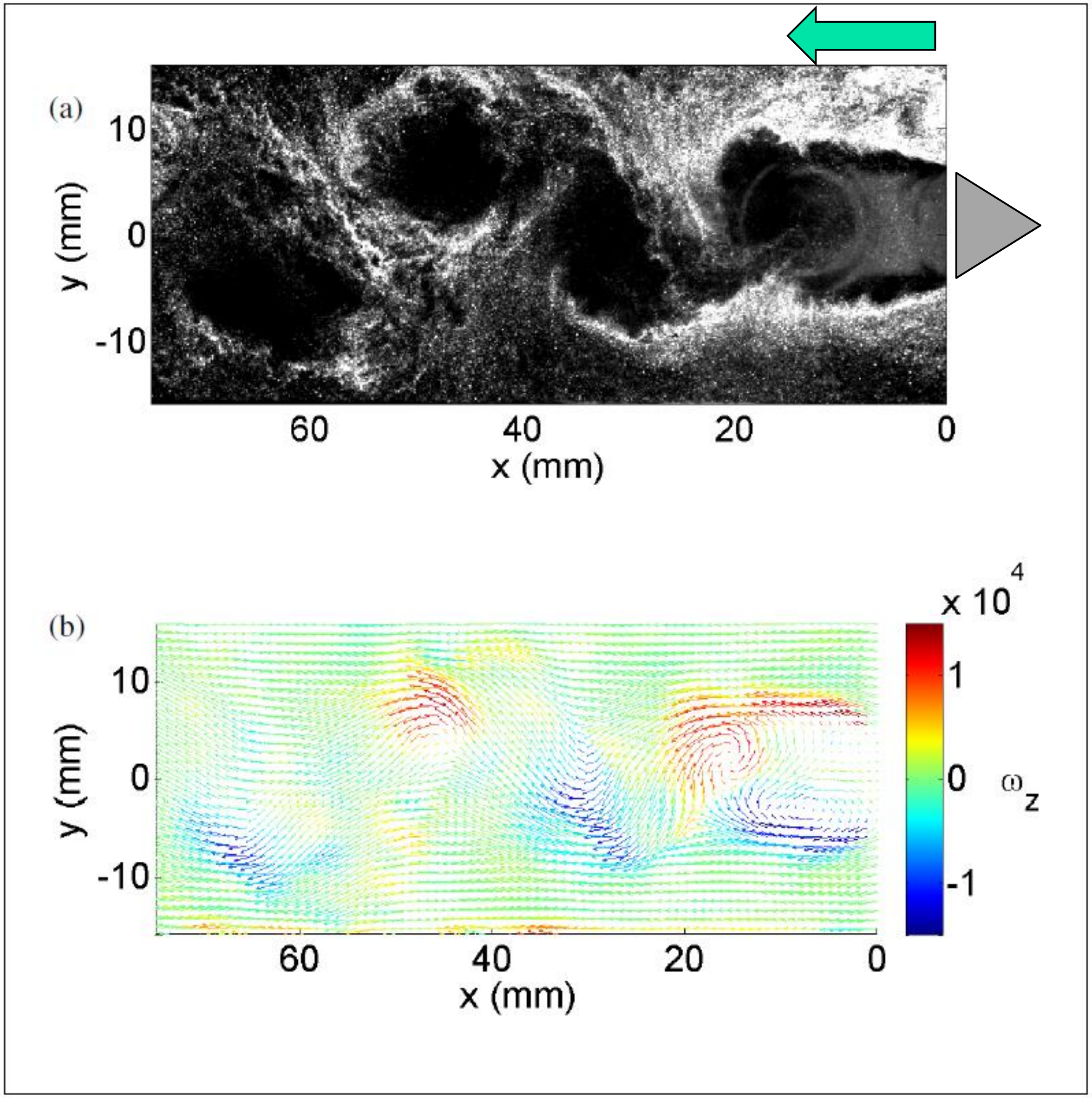

Characteristics of flows separated by bluff bodies: Reacting flows

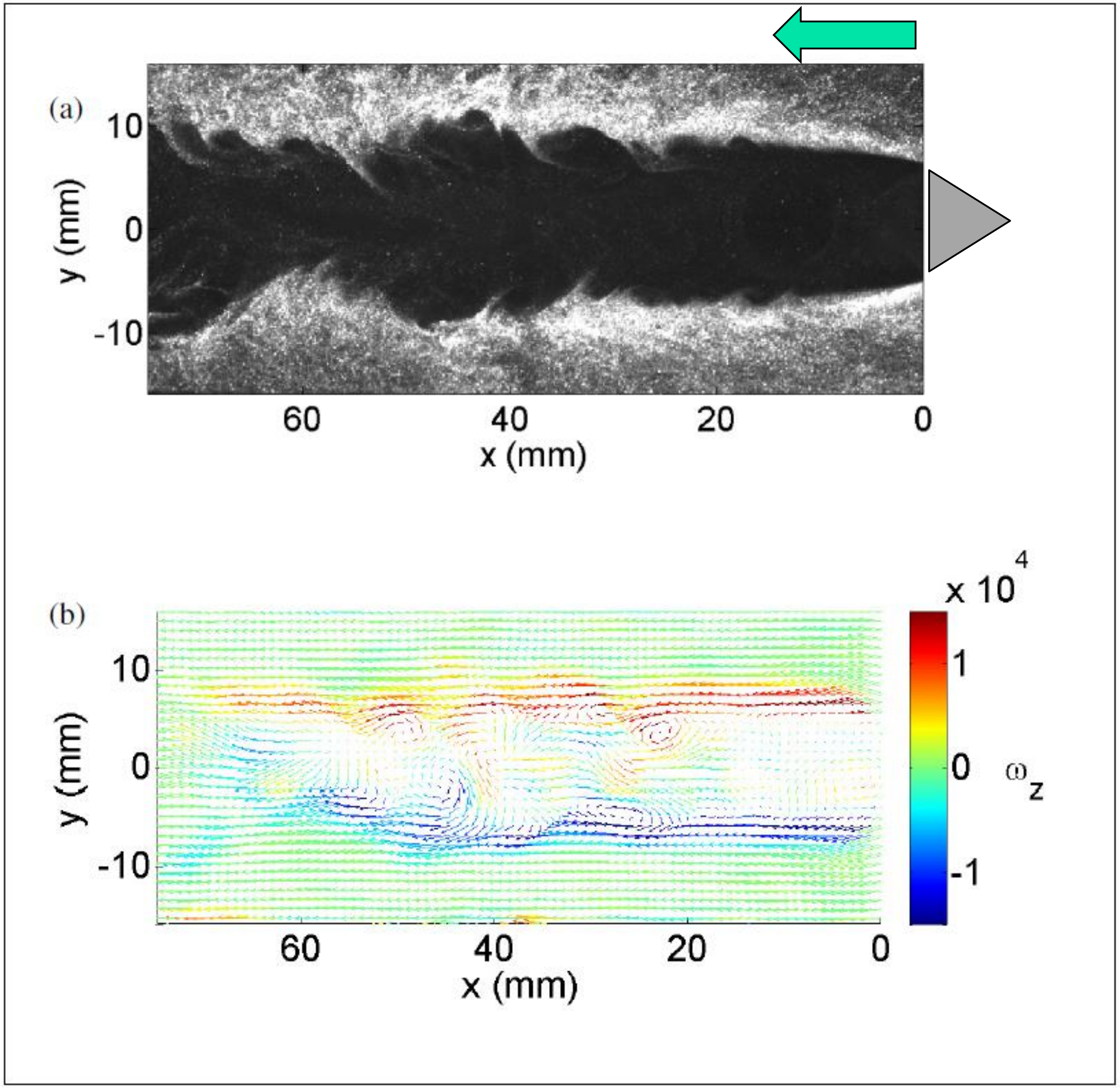

Effects of exothermicity

Results indicate substantially reduced turbulence intensities and vorticity magnitudes in combusting flows relative to the non-reacting flow for e.g. by Soteriou, Ghoniem (1994).

Fureby and Lofstrom (1994): vorticity field strength was much weaker and “less structured” (1994) in the presence of combustion.

Fuji and Eguchi (1981) and Bill and Tarabanis (1986) noted that turbulence levels in the reacting flow were much lower than the non-reacting case, particularly in the vicinity of the recirculation zone boundary.

The Vorticity Transport Equation

$$\frac{D\vec{\omega}}{Dt} = \underbrace{(\vec{\omega}.\vec{\nabla})\vec{V}}_{Vortex\ Stretching} - \underbrace{\vec{\omega}(\vec{\nabla}.\vec{V})}_{Gas\ Expansion} - \underbrace{\frac{\vec{\nabla}p \times \vec{\nabla}\rho}{\rho^2}}_{\substack{Baroclinic\\ Vorticity\\ Production}} + \underbrace{\vec{\nabla} \times \frac{\vec{\nabla}.\vec{\vec{S}}}{\rho}}_{Viscous Diffusion}$$

The kinematic gas viscosity , in term 4 rapidly increases through the flame, due to its larger temperature sensitivity. This substantially enhances the rate of diffusion and damping of vorticity, an effect emphasized by Coats (1996)

Term 3, i.e. the Baroclinic vorticity production, originates from the pressure and density gradient mismatch.

Term 2, i.e. dilatation also acts as a vorticity sink

Outline

Vast topic studied by combustion researchers for decades
Focus of premixed and to some extent on partially premixed flames.

1. Blowoff in Bluff Body Stabilized Premixed Flames

- Asses the developments in the field characterized by advent and implementation of sophisticated measurements.
- Nair and Lieuwen (2005-9s) used mie scattering and optical emission.
- Chaudhuri, Cetegen et al (2008-10s) used chemiluminescence imaging and simultaneous PIV PLIF.
- Kariuki, Mastorakos et al (2011-13s) used high speed PIV-PLIF.

2. Forced Blowoff, Vitiated (as in an afterburner) blowoff

3. Blowoff in Swirl Stabilized Flames

- Murgunandam, Seitzman (2005s) used chemiluminescence imaging; optical fiber coupled probes for control of blowoff
- Stoehr, Meier (2011s) used high speed PIV-PLIF.

4. Related Insights:

Near Blowoff Dynamics in Bluff Body Stabilized Flames

- Many researchers observed that near blowoff flames are highly unsteady and unstable (Zukoski (1958), Williams (1966) H.M. Nicholson (1948))
- Nicholson and Field (1948) described large scale pulsations in rich bluff body flames as they were blowing off.
- Observations of large scale, sinuous oscillations of a flame near blowoff were presented by Thurston (1958).
- Hertzberg et al. (1991) measured velocity fluctuations in a bluff body wake, indicating a growing amplitude of a relatively narrowband oscillation as blowoff was approached that they attributed to vortex shedding.
- A number of more recent studies by Nair and Lieuwen (2007), Kiel et al. (2007) and Erickson et al. have also noted these dynamics (2007).

Early views on blowoff

- Longwell (1953) suggested: blowoff due to imbalance in rate of entrainment of reactants (a PSR RZ)
- Insufficient heat supply by RZ to fresh gases (Williams GC, Hottel H. et al. 1951)
- Insufficient contact time of the fresh mixture in the shear layer with the burnt product in RZ. (Zukoski 1954)
- Extinction of a strained flamelet (Yamaguchi 1985)

- But these studies did not connect the early stages of blowoff dynamics with the final blowoff event as complete mechanism was lacking.

Blowoff Correlation

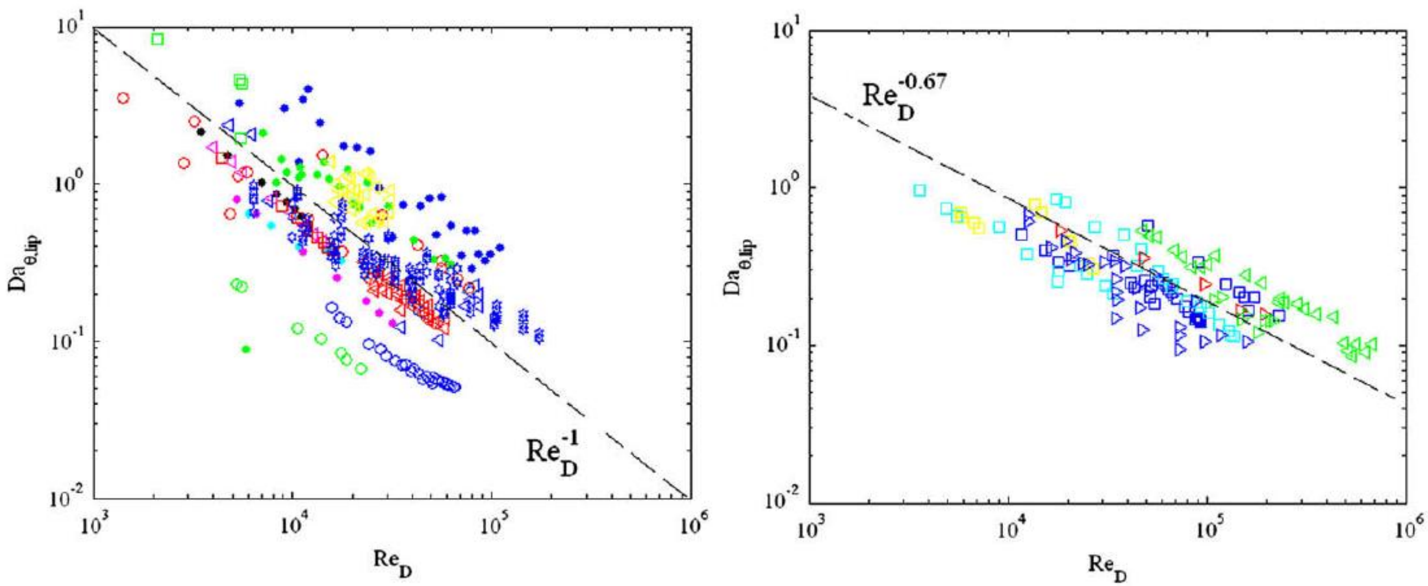

Correlation of two-dimensional (left) and axisymmetric (right) bluff body data sets showing Daq, lip at blowoff as a function of ReD utilizing T_PSR as the chemical time. (Shanbhogue 2009)

$$Da = bRe_D^a \Rightarrow \log(Da) = a\log(Re_D) + b$$

Summary of data used for data compilation reported (italicized and non-italicized text under "Bluff body type" denotes axisymmetric and nominally two-dimensional bluff body, respectively).

Reference	Symbol	Symbol color	Ref. year	U (m/s)	Re_D x1000	P (atm)	Inlet temp(K)	Fuel	Bluff body type
DeZubay [77]	□,□,□	Blue, cyan, yellow	1950	30–98	60–200	0.2–1	305	Propane	*Circular disk*
Plee and Mellor [80]	▷	Blue	1979	10–100	12–148	0.9	300	Propane	*Closed v-gutter*
C.R. King [140]	◁	Blue	1957	11–200	13–230	0.85	680	JP-4	Open v-gutter
Longwell et al. [141]	◁	Green	1948	72–254	223–782	1	422	Pentane	*Open v-gutter*
Zukoski [16]	○	Blue	1954	47–194	15–62	1	339	Gasoline	Cylinder
G. C. Williams [142]	●,○	Blue, red	1949	8–64	11–90	1	300	Propane	Cylindrical rod
Sanquer et al. [143]	□	Green	1998	2.9–7.6	2–6	1	280	Propane	Triangle, rectangle
Yamaguchi et al. [68]	●	Green	1985	8.5–39	12–52	1	295	Propane	Cylinder
Hottel et al. [78]	◁	Red	1962	40–82	12–63	0.4,0.6	394	Propane	Open v-gutter
Loblich [144]	●	Red	1962	9–80	4–36	1	293	Propane	Cylinder
Fetting [145]	●	Cyan	1958	10–100	4–26.5	1	300	Propane	Cylinder
Filippi [146]	●	Magenta	1960	10–100	4–26.5	1	300	Propane	Cylinder
Scurlock [147]	●	Yellow	1948	20–95	18–64	1	300	Propane	Cylinder
von Gerichten [92]	○	Green	1954	30–130	4.5–20	1	339	Gasoline	Cylinder
Ballal and Lefebvre [148]	▷	Red	1979	10–100	17–183	0.89	300	Propane	*Closed cone*
Hanna et al. [149]	▷	Green	1989	60–180	150–301	1	500	Diesel oil	*Closed cone*
Barrère and Mestre [95]	●	Black	1954	8–45	3–16	1	290	Propane	Cylinder
Barrère and Mestre [95]	◁	Magenta	1954	9–45	4–16	1	290	Propane	Open v-gutter
Barrère and Mestre [95]	□	Red	1954	10–45	5–16	1	290	Propane	Plate
Yang, Yen, and Tsai [97]	◁	Yellow	1994	14–27	15–31	0.99	298	LPG	Open v-gutter
Potter and Wong [74]	✡	Blue	1958	20–130	6.4–173	0.3–0.93	300	Propane	Cylinder

Shanbhogue et al (2009)

S. Shanbhogue, S. Hussain and T. Lieuwen, Progress in Energy and Combustion Dynamics, 2009

Works at Georgia Tech: Two stages of blowoff

Stage 1:

Initiation of flame hole, its convection downstream and healing. However the flame can persist indefinitely at this stage. This local extinction is hypothesized to be occurring at points where $k_{local} > k_{extinct}$

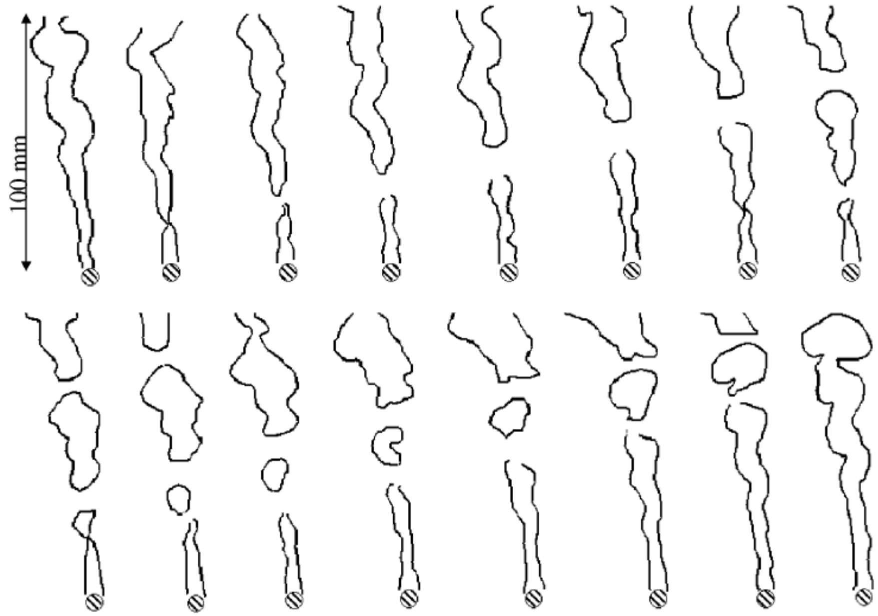

Sequence of flame images, 10 ms apart, taken during the first preblowoff stage at $\phi = 0.65$. Note presence of flame holes in the images (flow direction is from bottom to top). Nair and Lieuwen (2007)

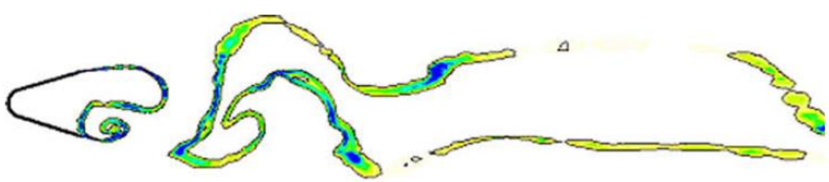

Computed reaction rate contours of a V-Gutter stabilized flame exhibiting localized extinction ($Re_D = 56{,}000$, $T_b/T_u = 2.9$) (Smith et al (2007)

S. Nair and T. Lieuwen, Journal of Propulsion and Power 2007

Stage 2:
Moments away from blowoff

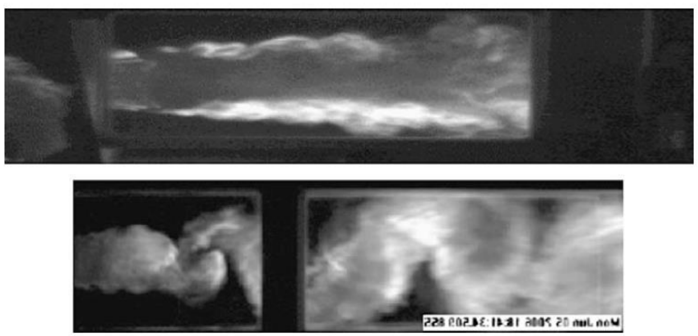

Measured high speed chemiluminescence images of V-gutter flames, at high equivalence ratio (ReD = 30,000, Tb/Tu = 5.9) (top) & close to blowoff (ReD = 35,000, Tb/Tu = 3) (below). Picture reproduced from Kiel et al (2007)

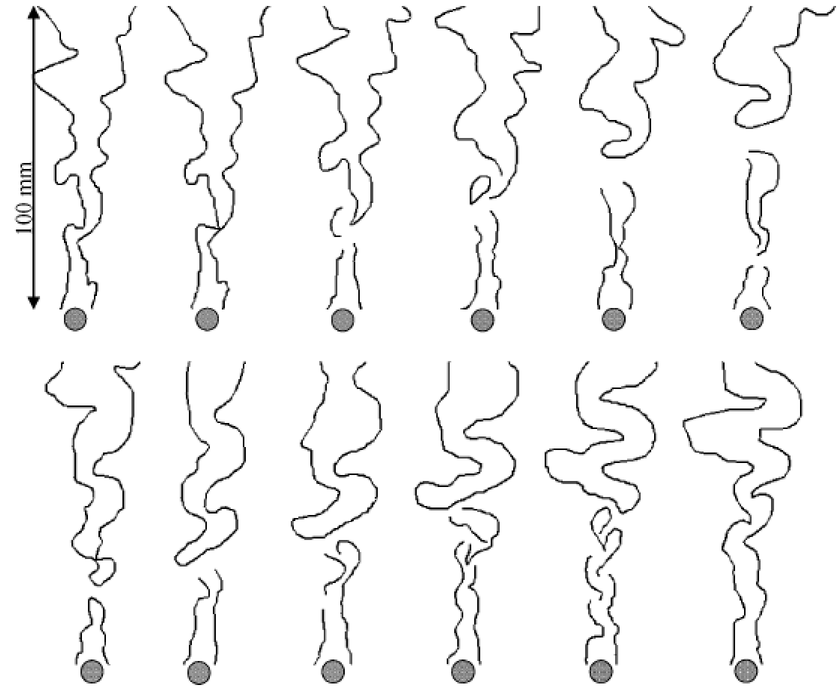

Sequence of flame images, 6 ms apart, taken during the second preblowoff stage at $\phi = 0.6$ (flow direction is from bottom to top)

Nair and Lieuwen (2007)

Return to asymmetry near blowoff

S. Nair and T. Lieuwen, Journal of Propulsion and Power 2007

Works at UConn with lean propane air flames

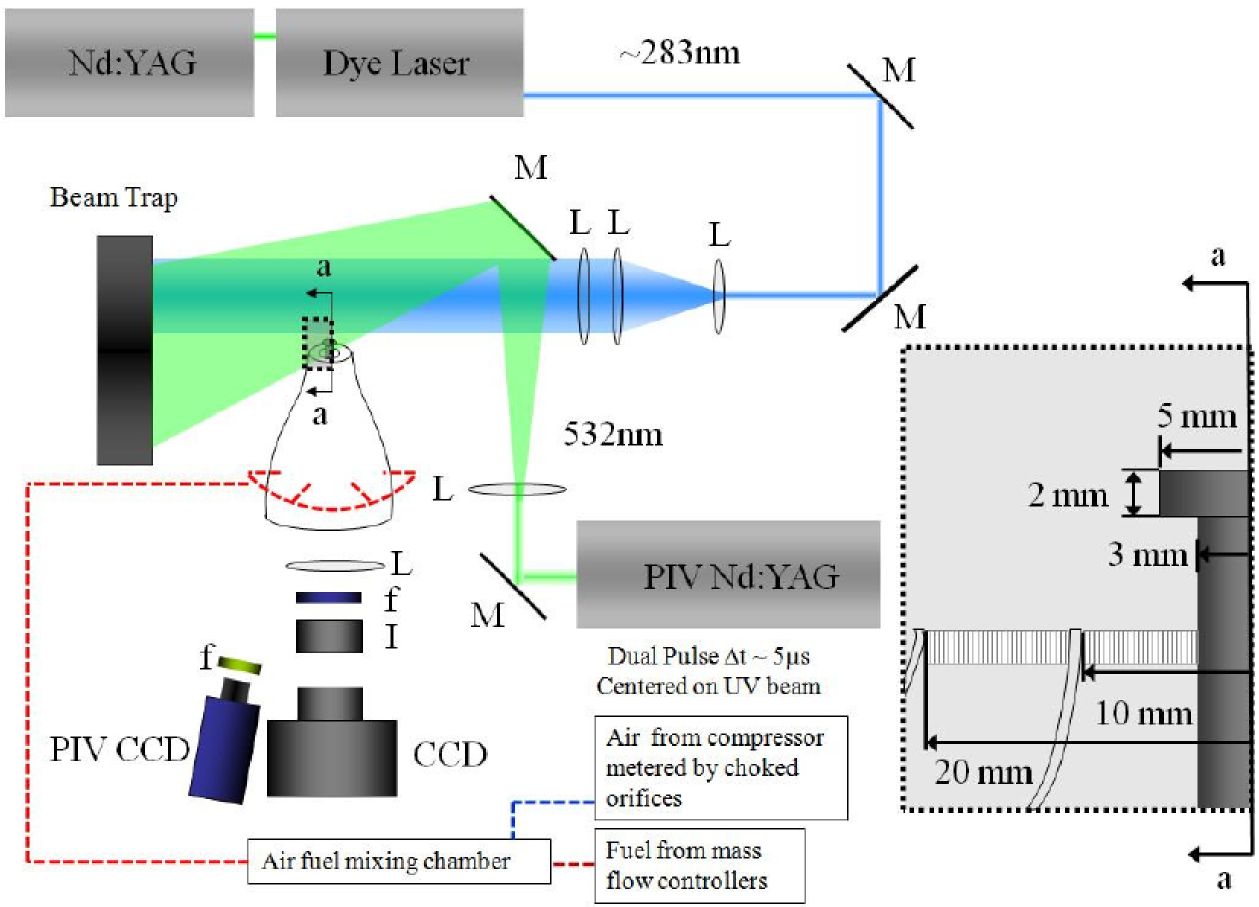

S. Chaudhuri, S. Kostka, M. Renfro, B. Cetegen, Combustion and Flame 2010

Laser Induced Fluorescence

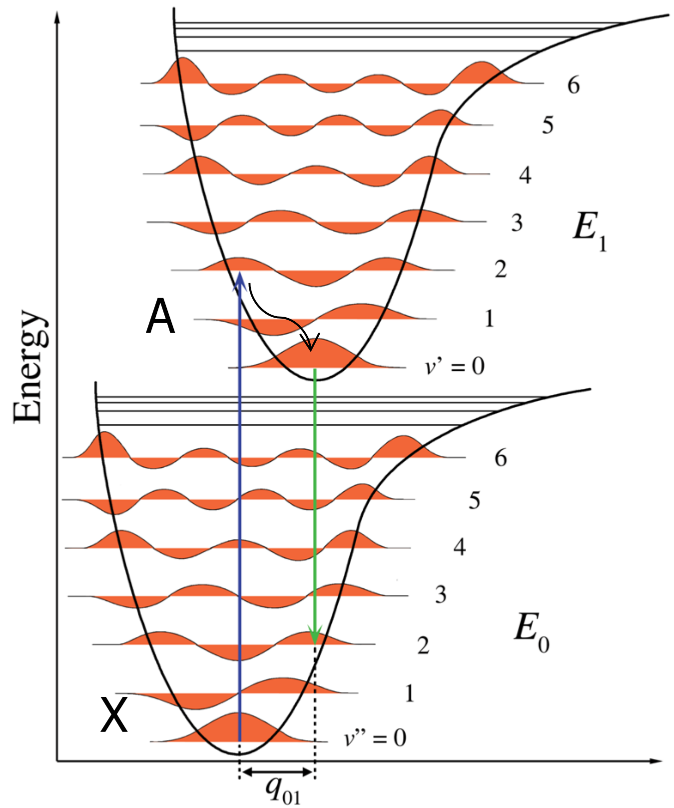

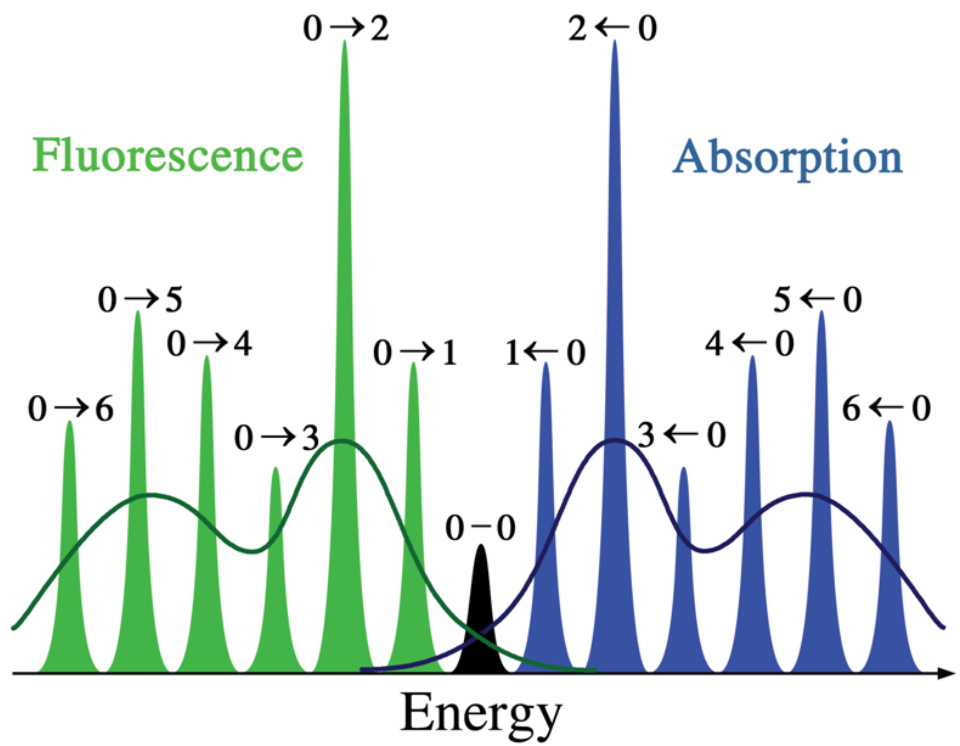

Fluorescence occurs at a low frequency than the incident radiation because the emissive transition occurs after some energy has been discarded into the surroundings.

Atkins Physical Chemistry 8th edition and Wikipedia

Single photon laser induced fluorescence species concentration detection: model

- Two level model:

b_{12} and b_{21} :rate constants for absorption and stimulated emission and are related to the Einstein coefficients by

$$b = \frac{BI_\upsilon}{c}$$

$$\frac{dN_1}{dt} = \dot{N}_1 = -N_1 b_{12} + N_2 (b_{21} + A_{21} + Q_{21})$$

$$\frac{dN_2}{dt} = \dot{N}_2 = N_1 b_{12} - N_2 (b_{21} + A_{21} + Q_{21} + P + W_{2i})$$

b, A , Q, P, W are termed rate constants

A = Einstein A coefficient

P = Predissociation rate constant

W_{2i} = photoionization rate constant

Q = collisional quenching rate.

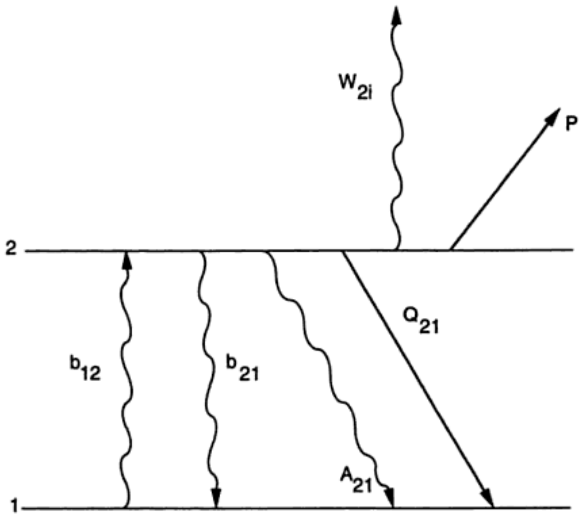

Fig 7. Simple two energy level diagram for LIF modelling. from [1]

From Laser Diagnostics in Combustion by Alan C. Eckbreth

… continued

Neglecting predissociation and photoionization we get

$$\frac{dN_1}{dt} + \frac{dN_2}{dt} = 0$$

$$\therefore N_1 + N_2 = N_1^0 = cons. = \textbf{species population prior to excitation}$$

The Flouroscence signal is proportional to $\boldsymbol{N_2 A_{21}}$ and hence we need to relate

$$N_2 \rightarrow N_1^0$$

This is done by eliminating N_1 from the N_2 rate equation and integrating we get:

$$N_2(t) = \frac{b_{12} N_1^0}{r}\left(1 - e^{-rt}\right)$$

where $r = b_{12} + b_{21} + A_{21} + Q_{21}$

and $N_2(t=0) = 0$

… continued

$$N_2(t) = \frac{b_{12} N_1^0}{r}$$ at steady state

$$F = h\upsilon N_2 A_{21} \frac{\Omega}{4\pi} lA \sim N_1^0 \frac{B_{12}}{B_{12}+B_{21}} \frac{A_{21}}{1+\frac{I_{sat}^{\upsilon}}{I_{\upsilon}}}$$

$$I_{sat}^{\upsilon} = \frac{(A_{21}+Q_{21})c}{B_{12}+B_{21}}$$ Saturation spectral intensity

$$F \sim N_1^0 \frac{B_{12} I_{\upsilon}}{B_{12}+B_{21}} \frac{A_{21}}{A_{21}+Q_{21}} \text{..........} for \ldots I_{\upsilon} << I_{sat}^{\upsilon}$$

$$F \sim N_1^0 \frac{B_{12}}{B_{12}+B_{21}} A_{21} \text{....................} for \ldots I_{\upsilon} >> I_{sat}^{\upsilon}$$

From Laser Diagnostics in Combustion by Alan C. Eckbreth

Particle Image Velocimetry

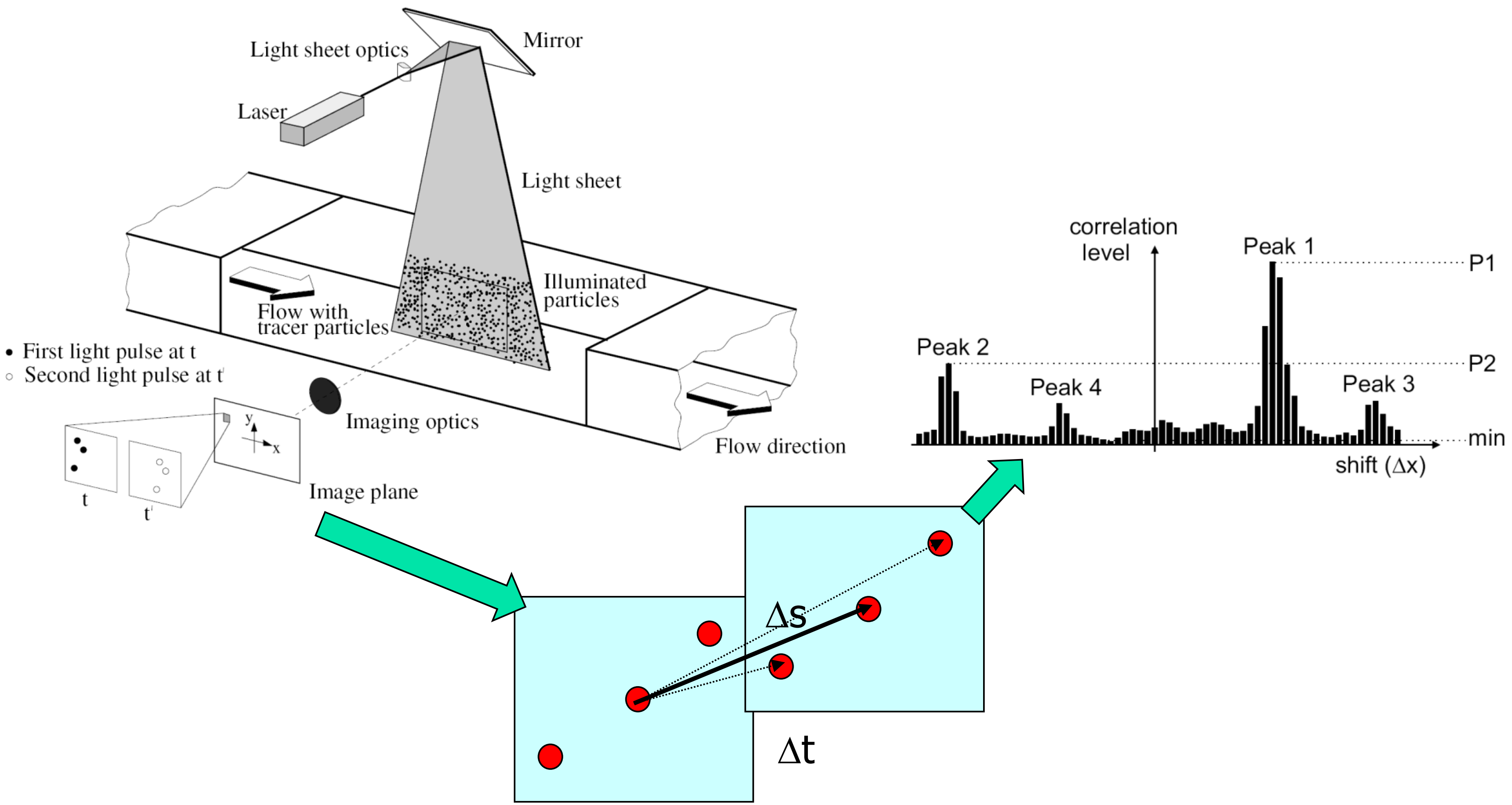

Raffell, Willert, Wereley, Kompenhans: Particle Image Velocimetry, Springer

Time resolved chemiluminescence imaging

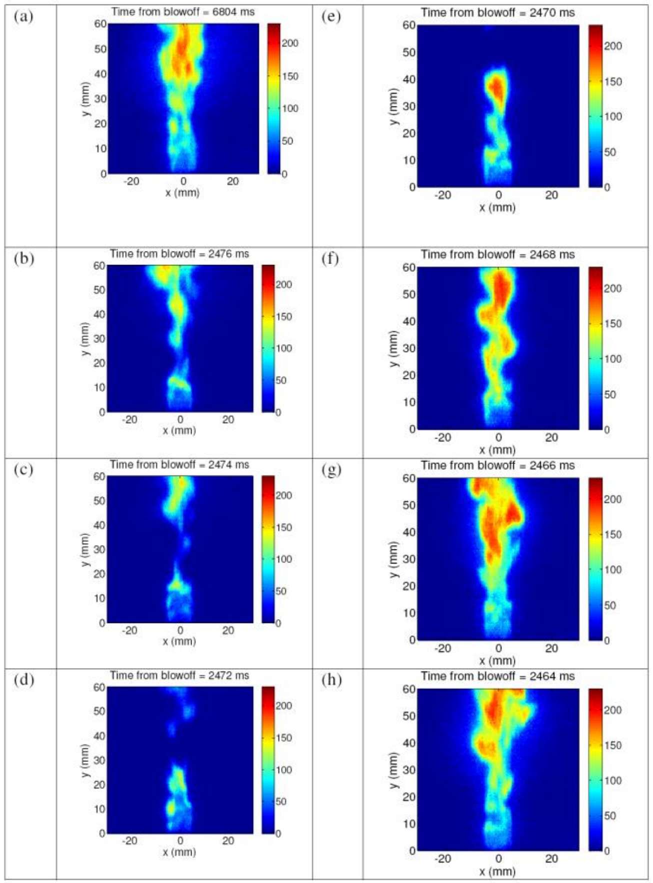

Near blowoff symmetric and asymmetric modes

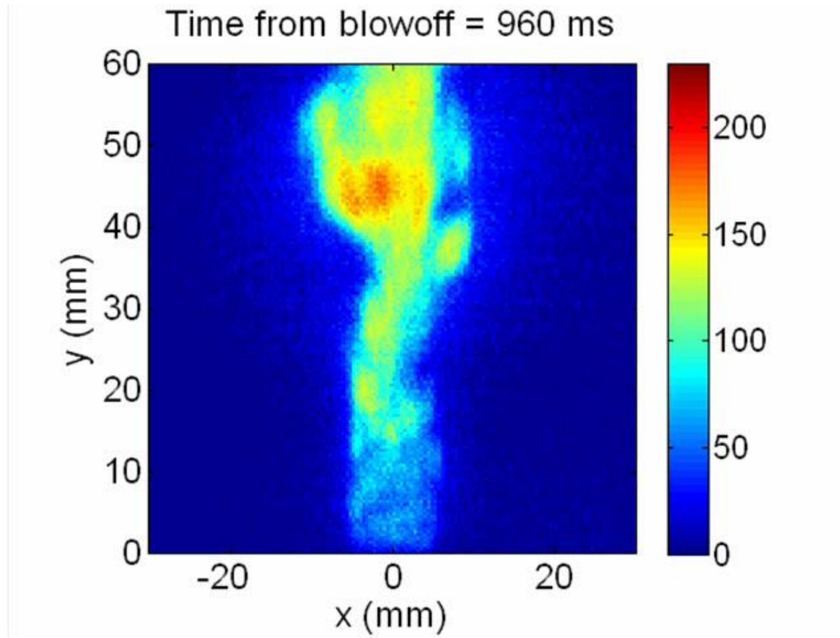

Extinction and Reignition

Blowoff

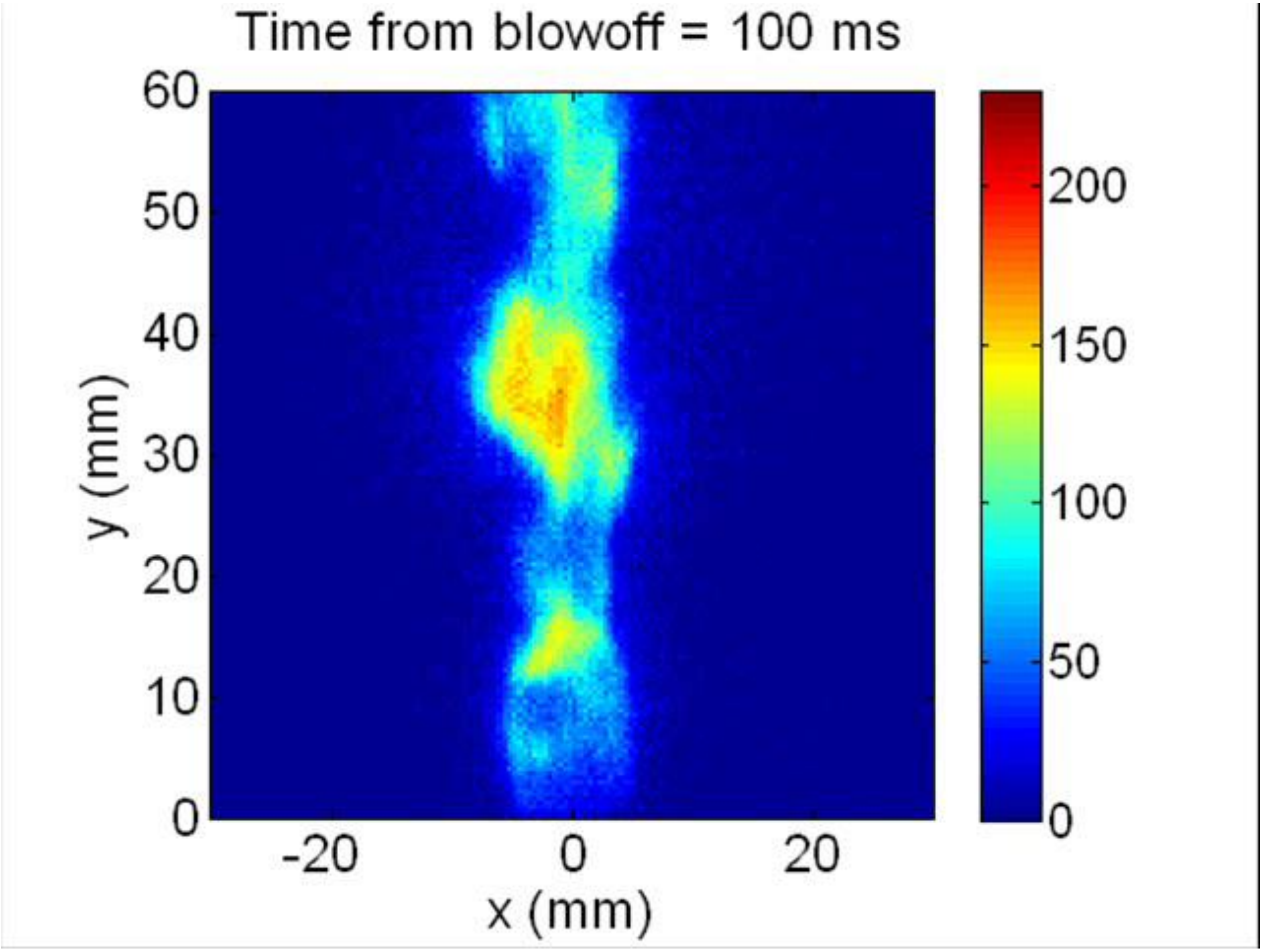
Time from blowoff = 100 ms
y (mm)
x (mm)
60
50
40
30
20
10
0
-20
0
20
200
150
100
50
0

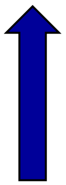

Simultaneous PIV and OH PLIF

Stable flame at
$\phi = 0.9$

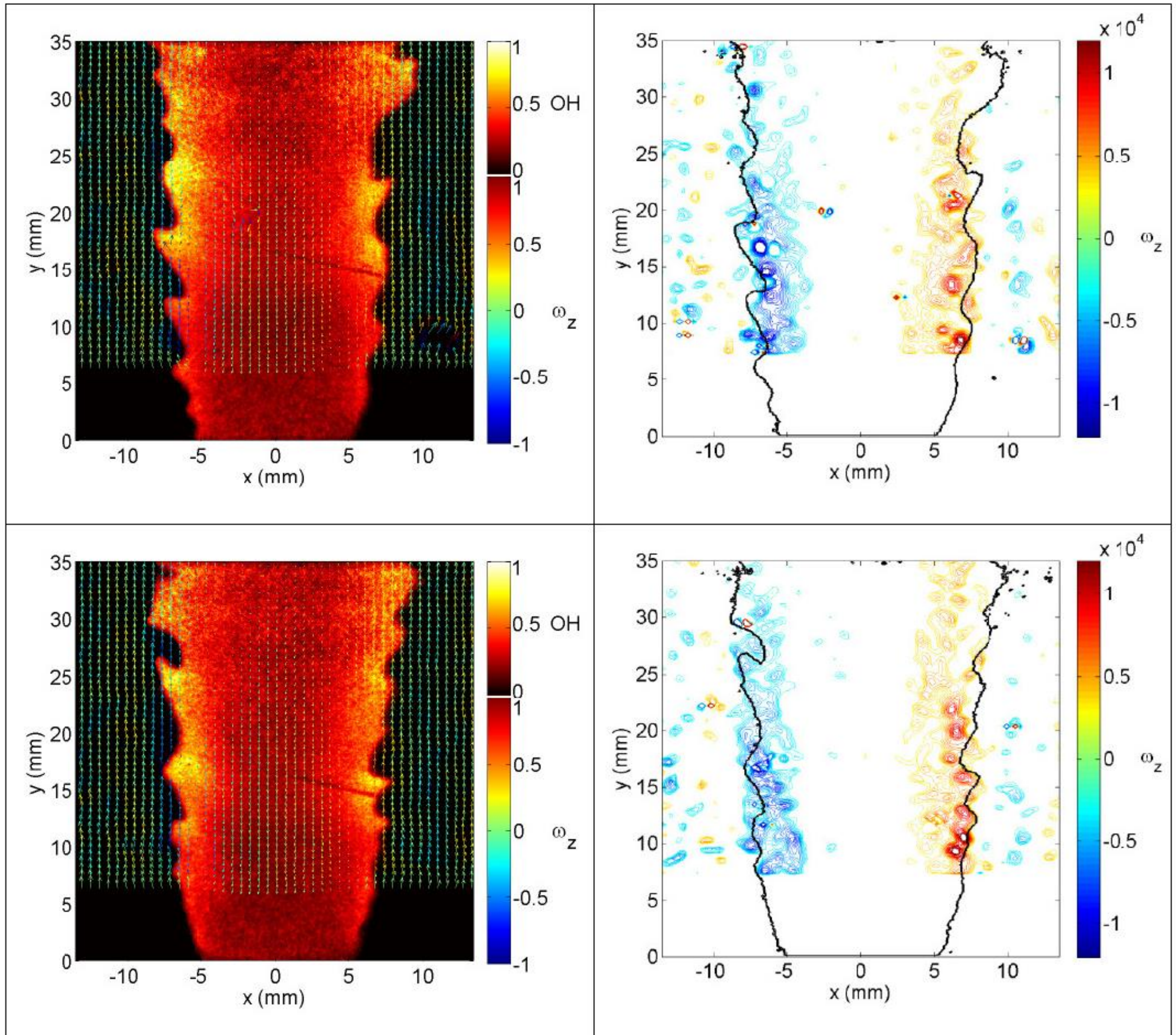

S. Chaudhuri, S. Kostka, M. Renfro, B. Cetegen, Combustion and Flame 2010

… continued

Unstable flame at
ϕ= 0.775 near blowoff

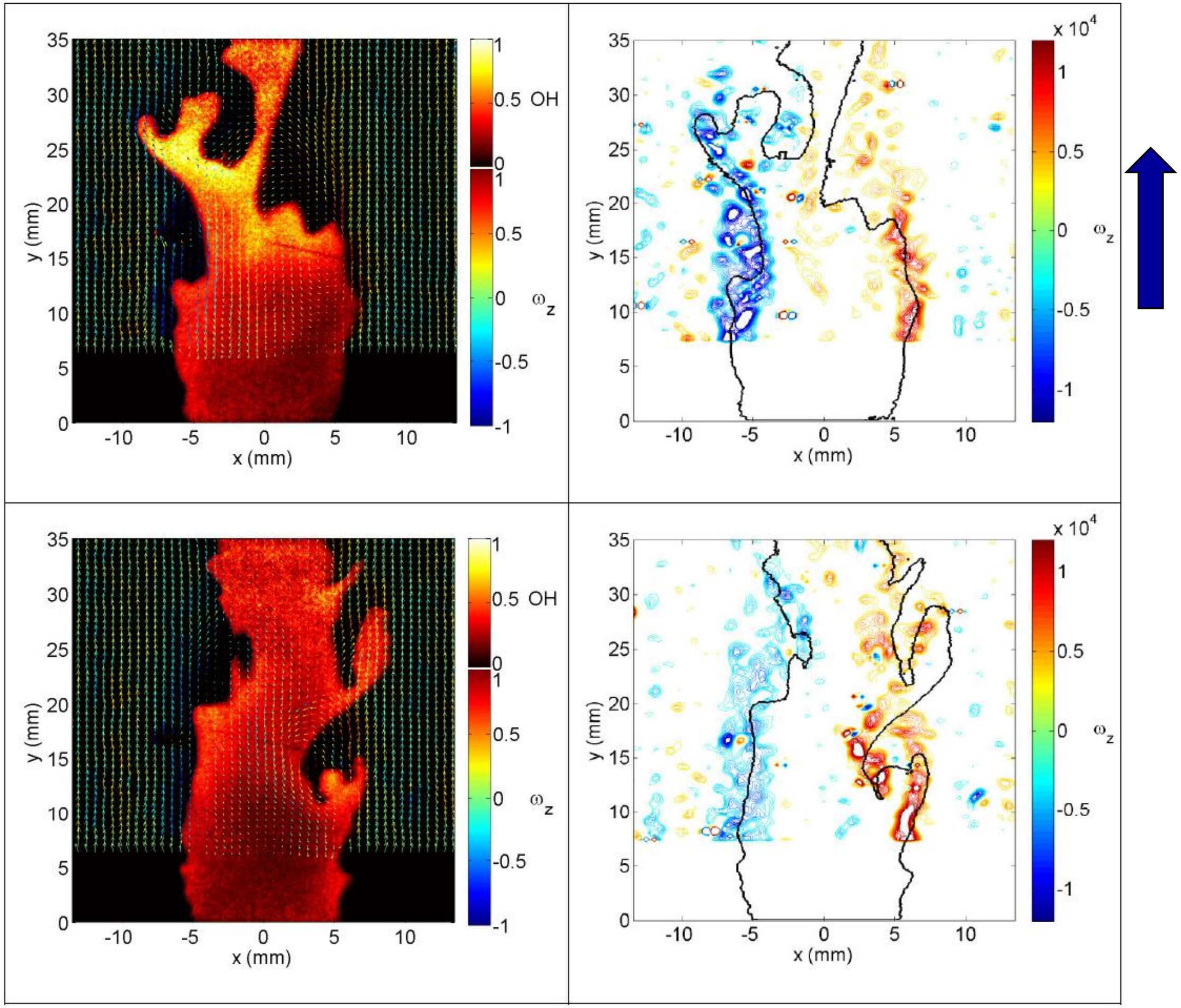

Unstable flame at ϕ= 0.77 near blowoff

Extinction along shear layers

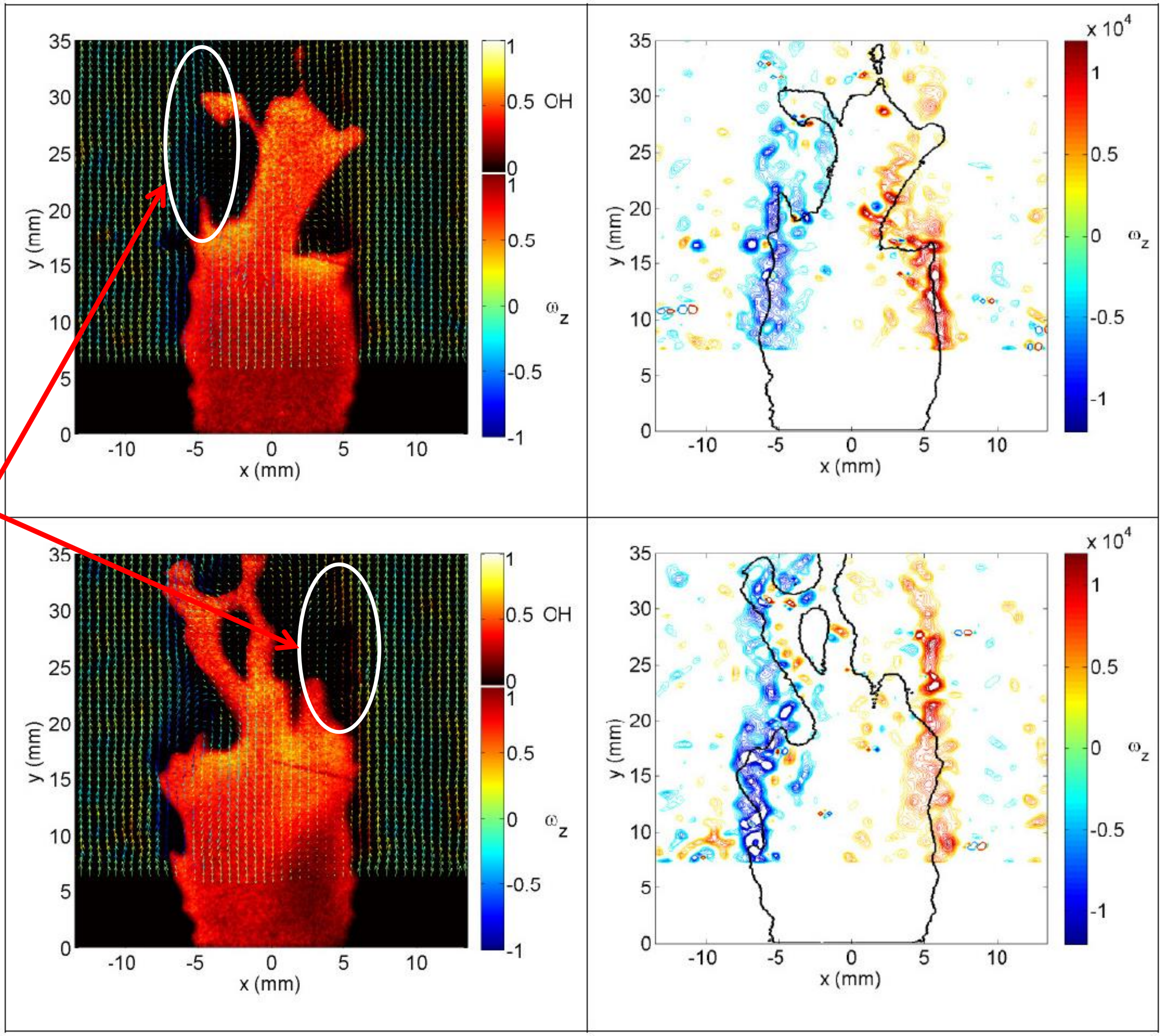

S. Chaudhuri, S. Kostka, M. Renfro, B. Cetegen, Combustion and Flame 2010

Mean U_y and ω_z superimposed with OH-PLIF

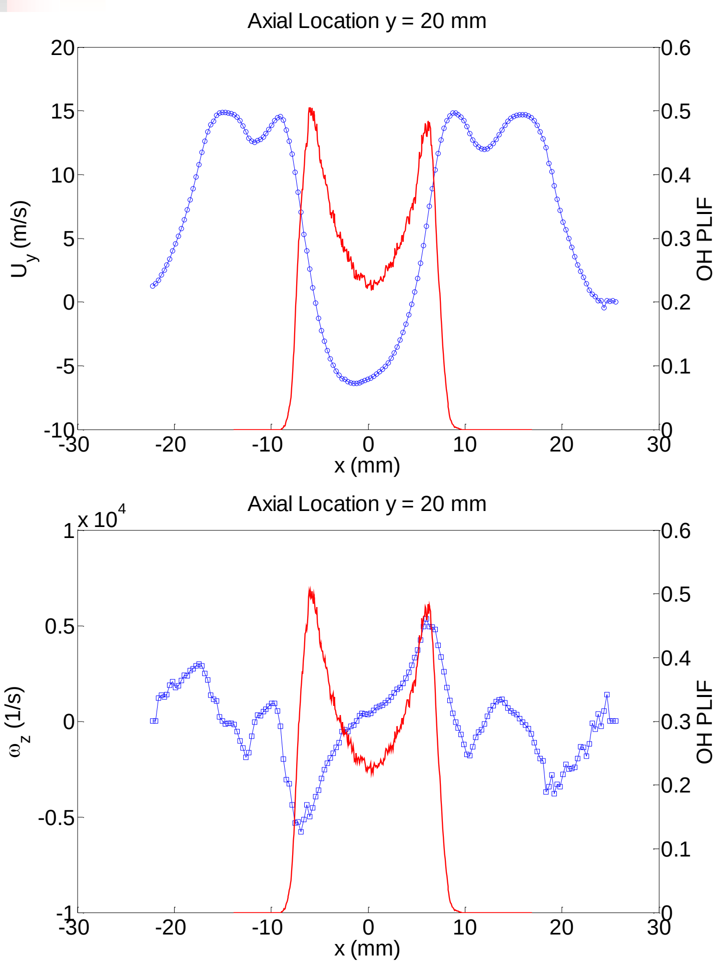

ϕ = 0.90 : Far from blowoff

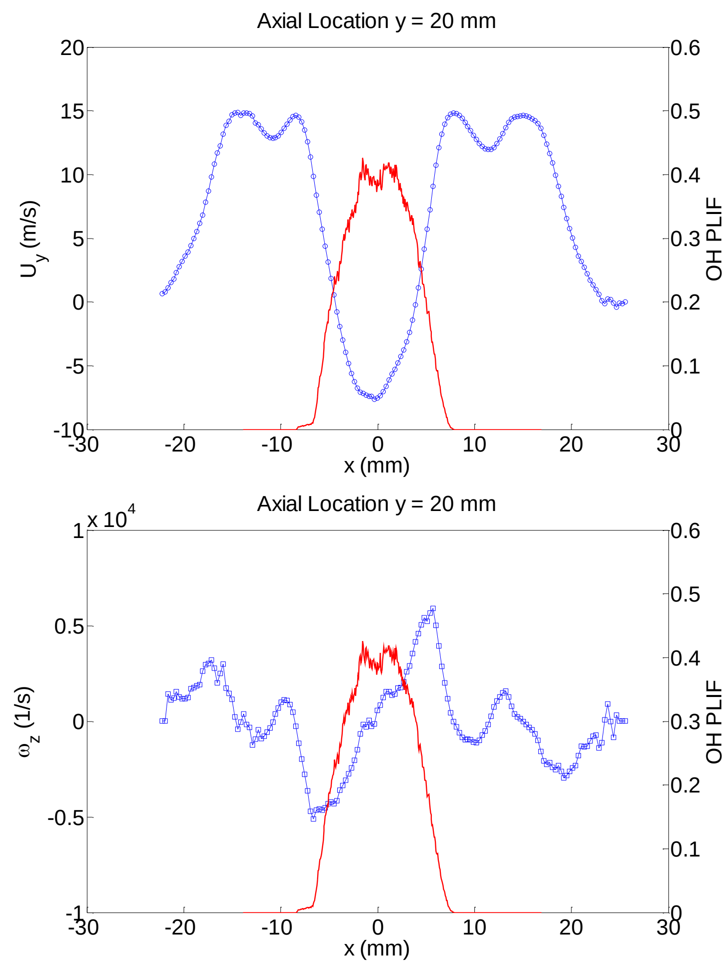

ϕ = 0.77 : Near blowoff

Mean U_y and ω_z superimposed with OH-PLIF

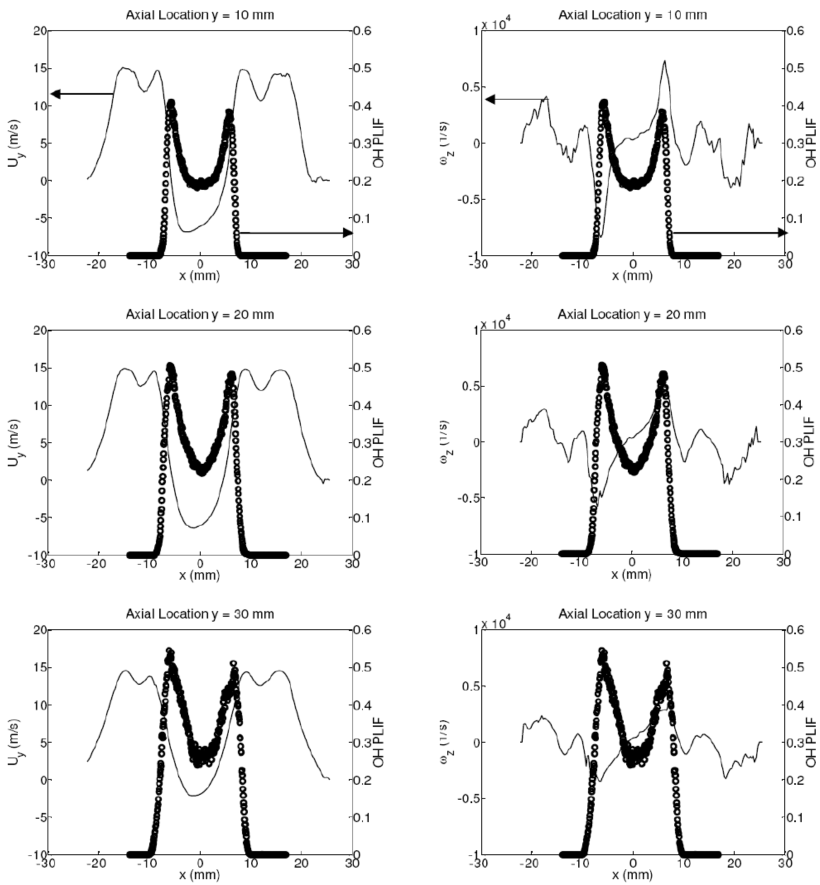

$\phi = 0.90$

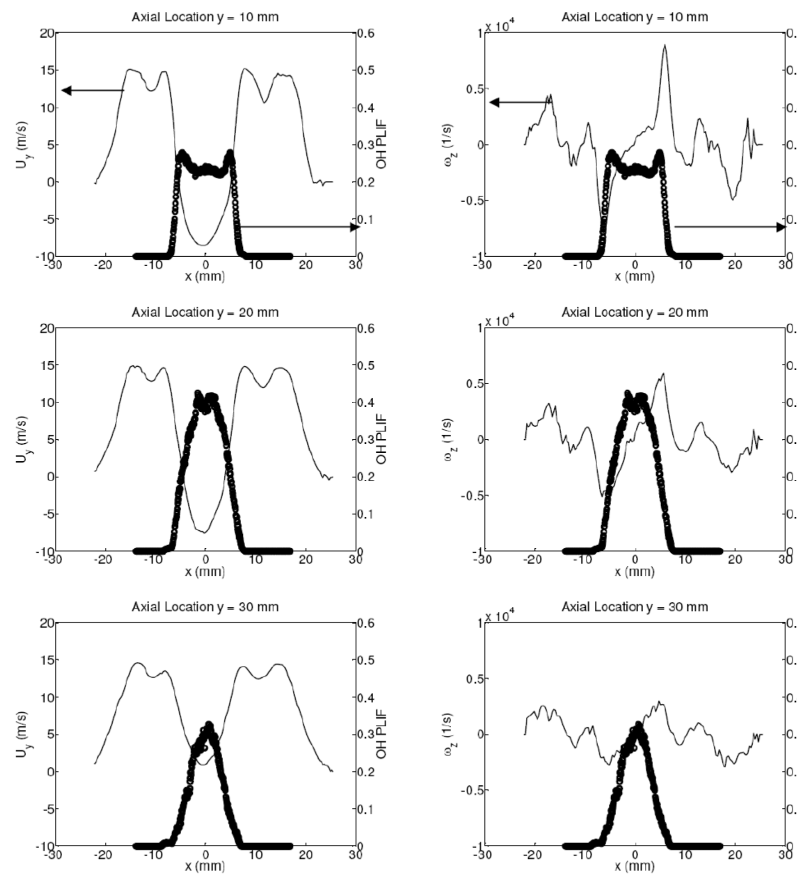

$\phi = 0.77$

S. Chaudhuri, S. Kostka, M. Renfro, B. Cetegen, Combustion and Flame 2010

Conditional pdfs : pdf(|ω| |OH)

ϕ = 0.90

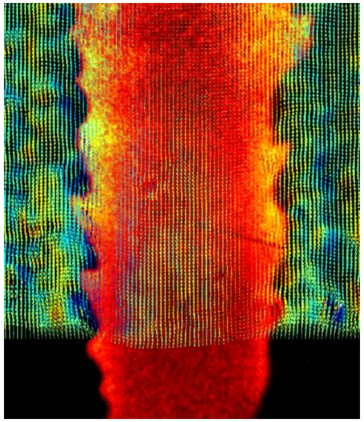

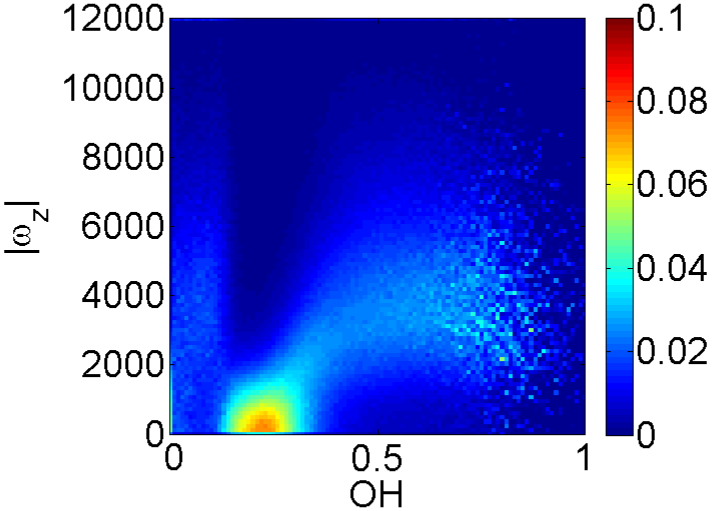

ϕ = 0.77

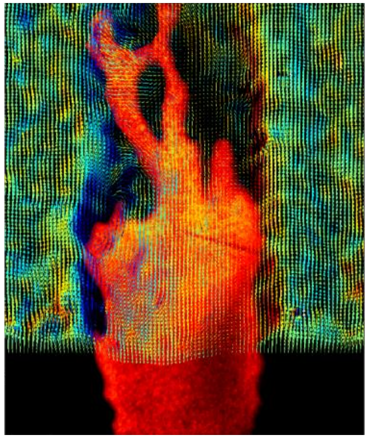

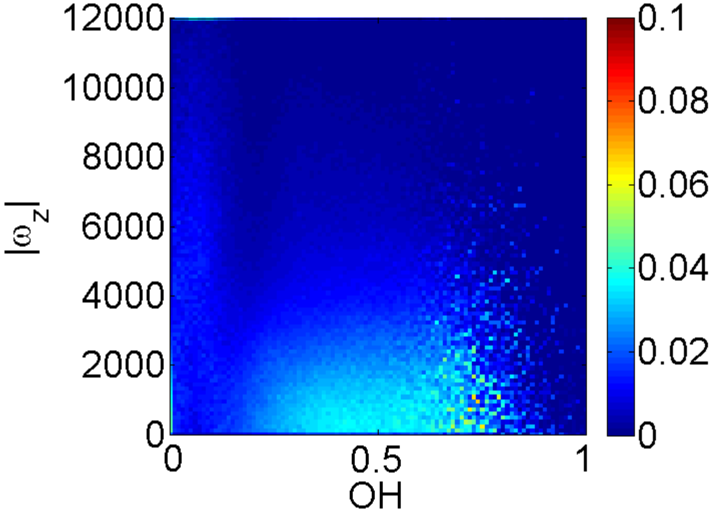

S. Chaudhuri, S. Kostka, M. Renfro, B. Cetegen, Combustion and Flame 2010

Basics of Premixed Flame Extinction

1. Extinction by volumetric heat loss
2. Extinction by stretch
   a. Le > 1
   b. Le < 1

$$\rho_u s_L \frac{\mathrm{d}T}{\mathrm{d}x} = \frac{\mathrm{d}}{\mathrm{d}x}\left(\frac{\lambda}{c_p}\frac{\mathrm{d}T}{\mathrm{d}x}\right) + \frac{Q}{c_p}\omega - \alpha(T - T_u).$$

$$M = \frac{s_L}{s_{L,\mathrm{ref}}}.$$

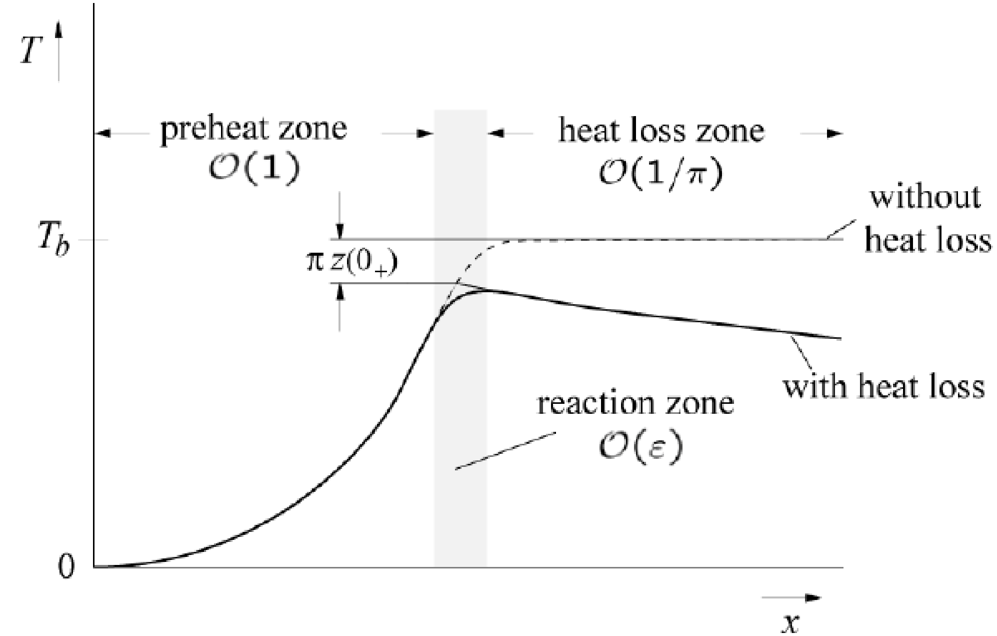

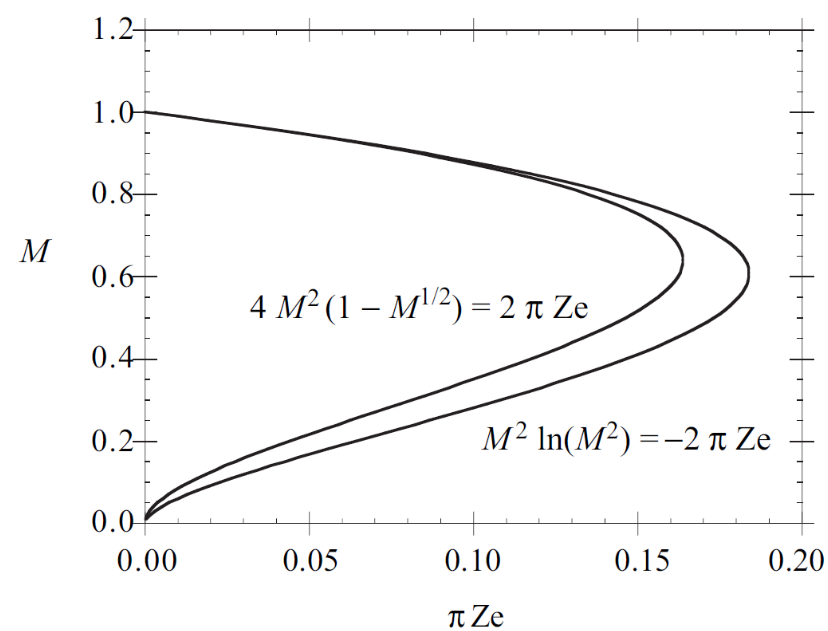

Peters Summer school lecture notes 2010

Flame Stretch

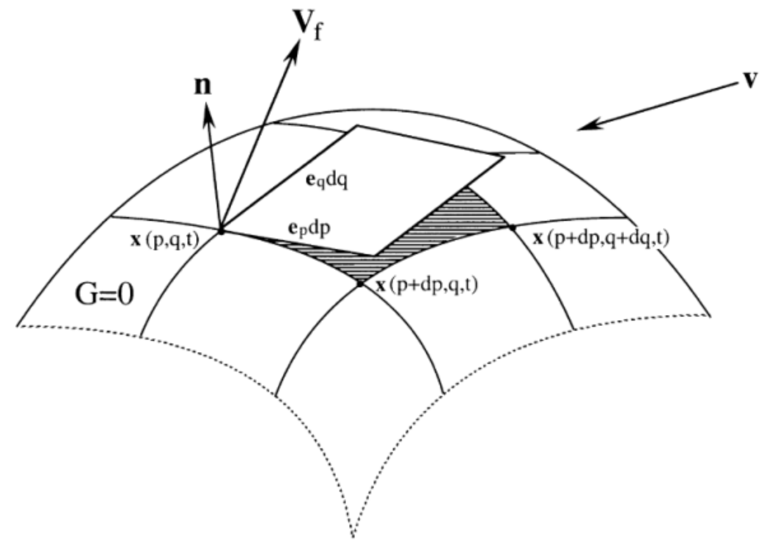

generalized form of flame stretch

$$\kappa = \frac{1}{A}\frac{dA}{dt} = \overbrace{\underbrace{S_L c}_{\text{stretch rate by pure curvature}} - \underbrace{(\mathbf{v}\cdot\mathbf{n})c}_{\text{normal strain } \kappa_n}}^{\text{stretch rate by curvature}} + \underbrace{\nabla_t \cdot \mathbf{v}_t}_{\text{tangential strain } \kappa_s}$$

Tangential straining part of flame:

$$\kappa_s = \left(\delta_{ij} - n_i n_j\right) S_{ij}$$

$$\kappa_{s,2D} = -n_x \times n_y \times \left(\frac{\partial u}{\partial y} + \frac{\partial v}{\partial x}\right) + \left(1 - n_x^2\right) \times \frac{\partial u}{\partial x} + \left(1 - n_y^2\right) \times \frac{\partial v}{\partial y}$$

C.K. Law and C.J. Sung: Progress in Energy and Combustion Science 26 (2000) 459–505

Stretch Effects

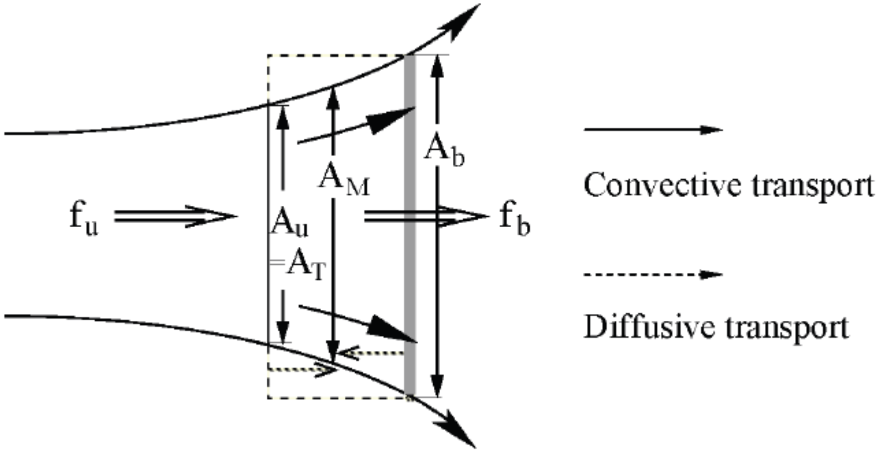

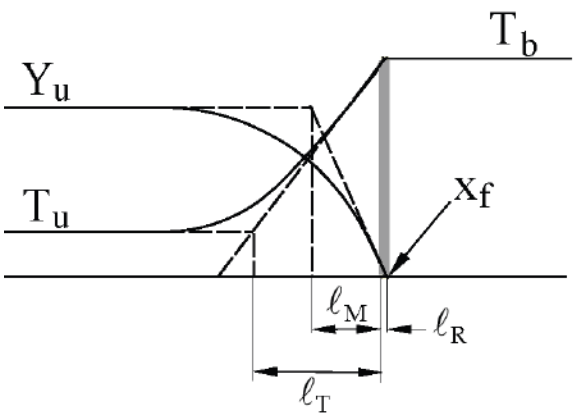

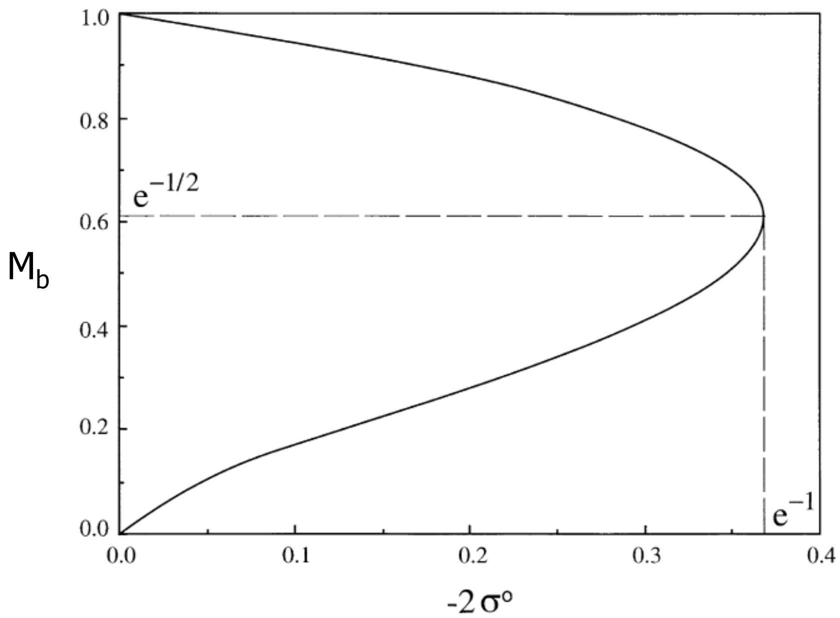

$$M_b^{\,2}\ln M_b^{\,2} = 2\sigma^0$$

$$\textit{where}\quad \sigma^0 = \frac{Ze^0}{2}\left(\frac{1}{Le} - 1\right)Ka^0$$

$$Ze = \frac{E_a}{R^0 T^2_{\max}}$$

$$Le = \frac{\alpha}{D}$$

$$Ka = \frac{l_T}{S_u}\kappa$$

All HC flames except methane are Le>1

Mean pdfs of strain rate along OH PLIF edge

ϕ = 0.90

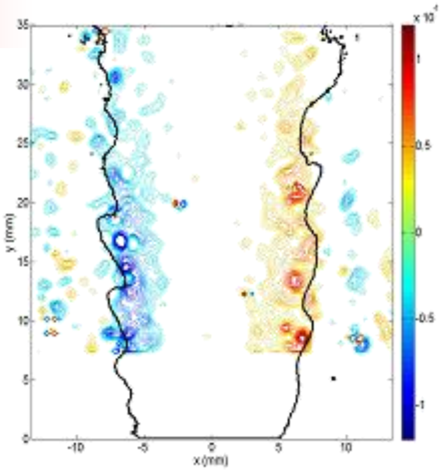

ϕ = 0.77

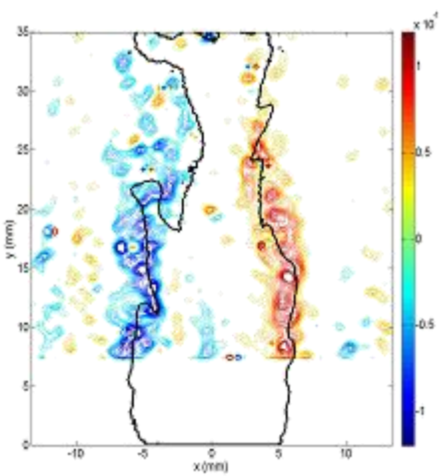

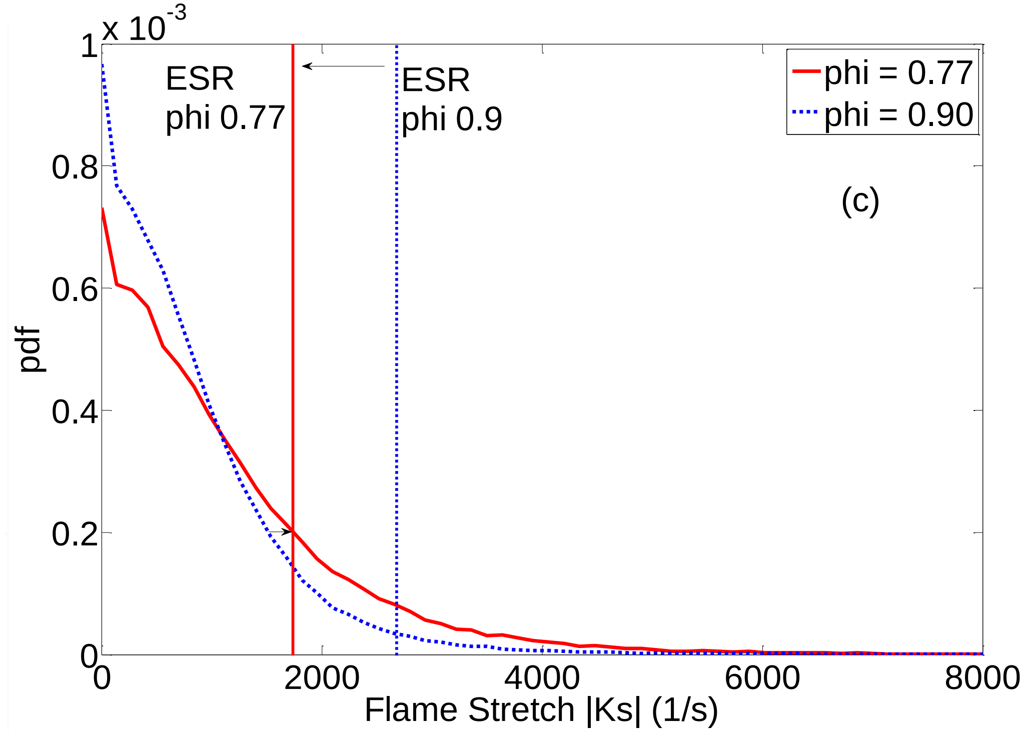

Limiting condition created by κ_{flame} and κ_{esr} shifting in opposite directions with reducing ϕ.

S. Chaudhuri, S. Kostka, M. Renfro, B. Cetegen, Combustion and Flame 2010

Stage 3 in blowoff dynamics

Recirculation zone burn

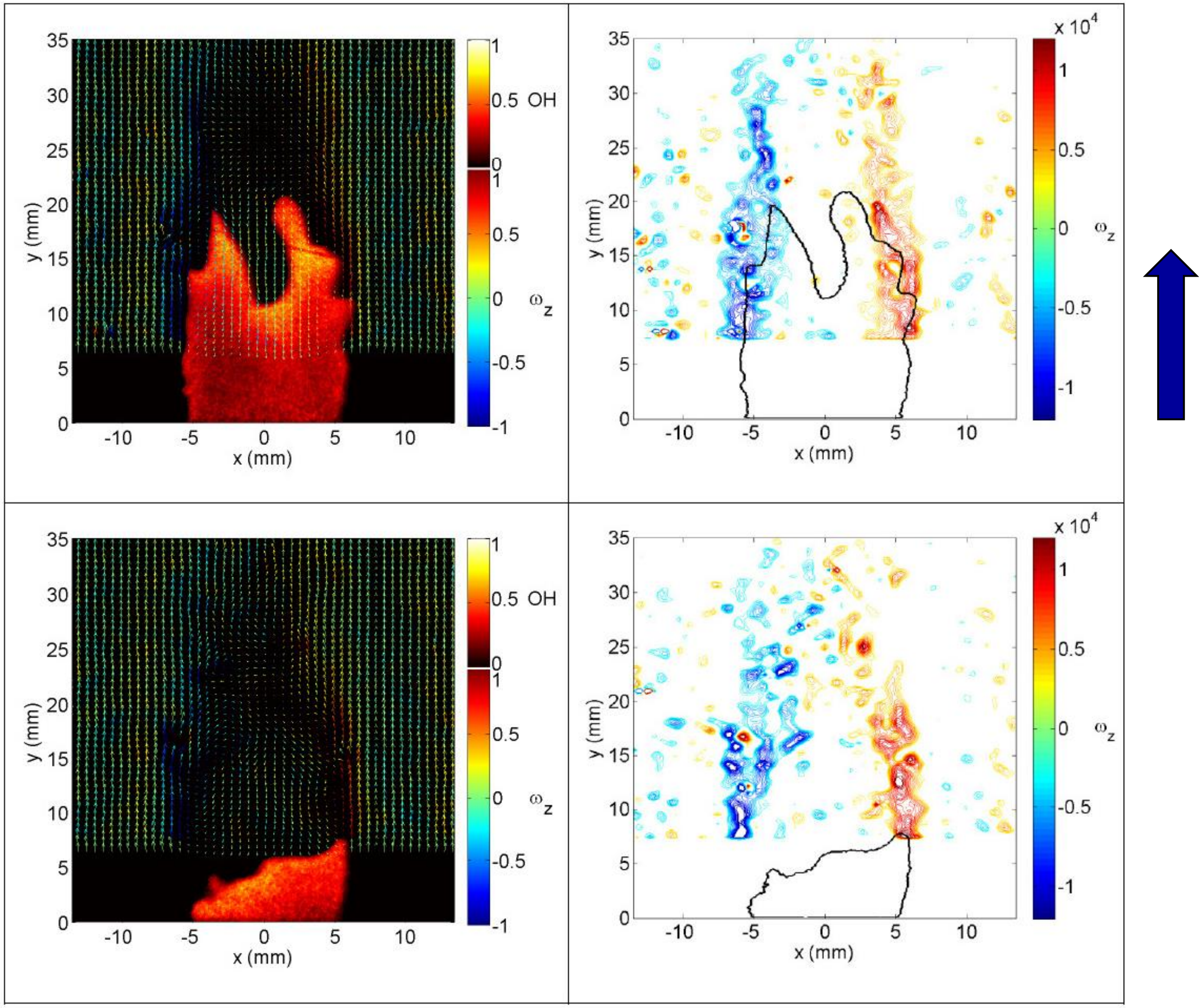

S. Chaudhuri, S. Kostka, M. Renfro, B. Cetegen, Combustion and Flame 2010

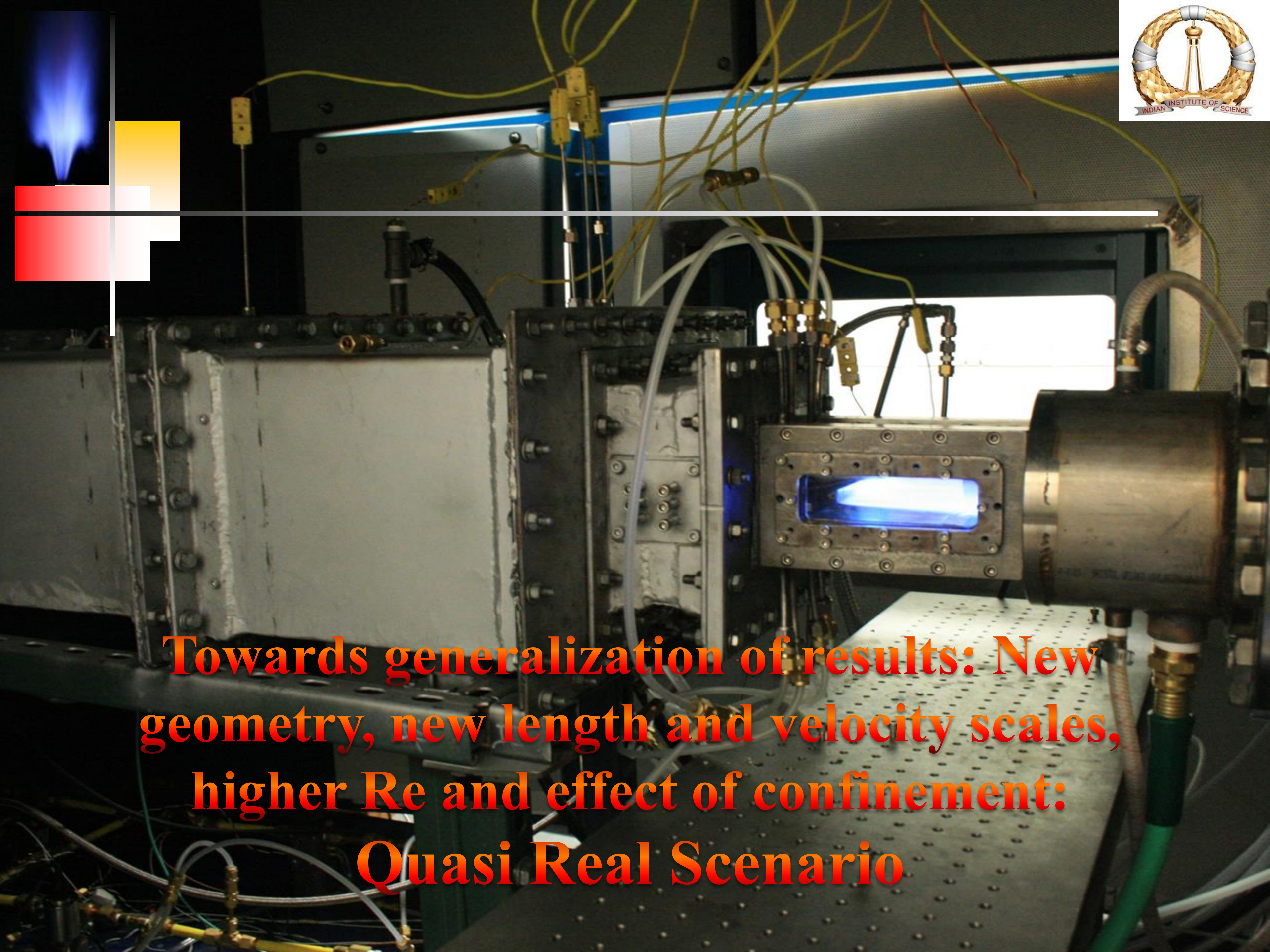

Towards generalization of results: New geometry, new length and velocity scales, higher Re and effect of confinement: Quasi Real Scenario

The UConn Rig

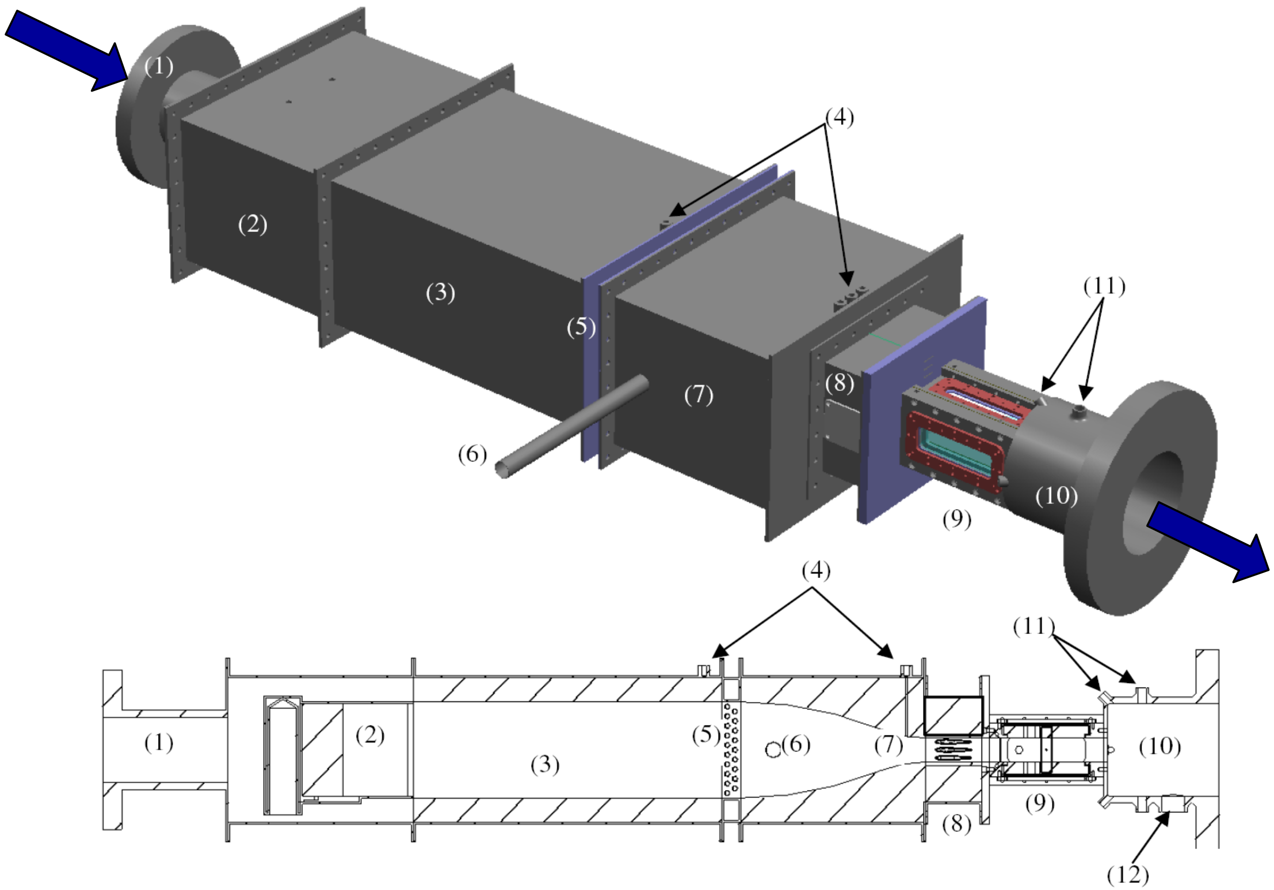

Layout of experimental rig. (1): Air inlet, (2): Maxon NP-LE burner, (3): Settling Duct, (4): Thermocouple Ports, (5): Heat exchanger, (6): PIV-Seeded air inlet, (7): Convergent nozzle, (8): Fuel injectors, (9): Optically accessible test burner, (10): Dump duct, (11): Water nozzle ports, (12): Water drain. (image courtesy: Steven Tuttle)

Experimental Setup

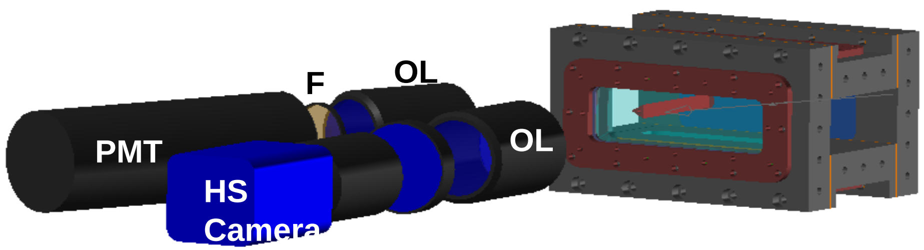

Imaging setup

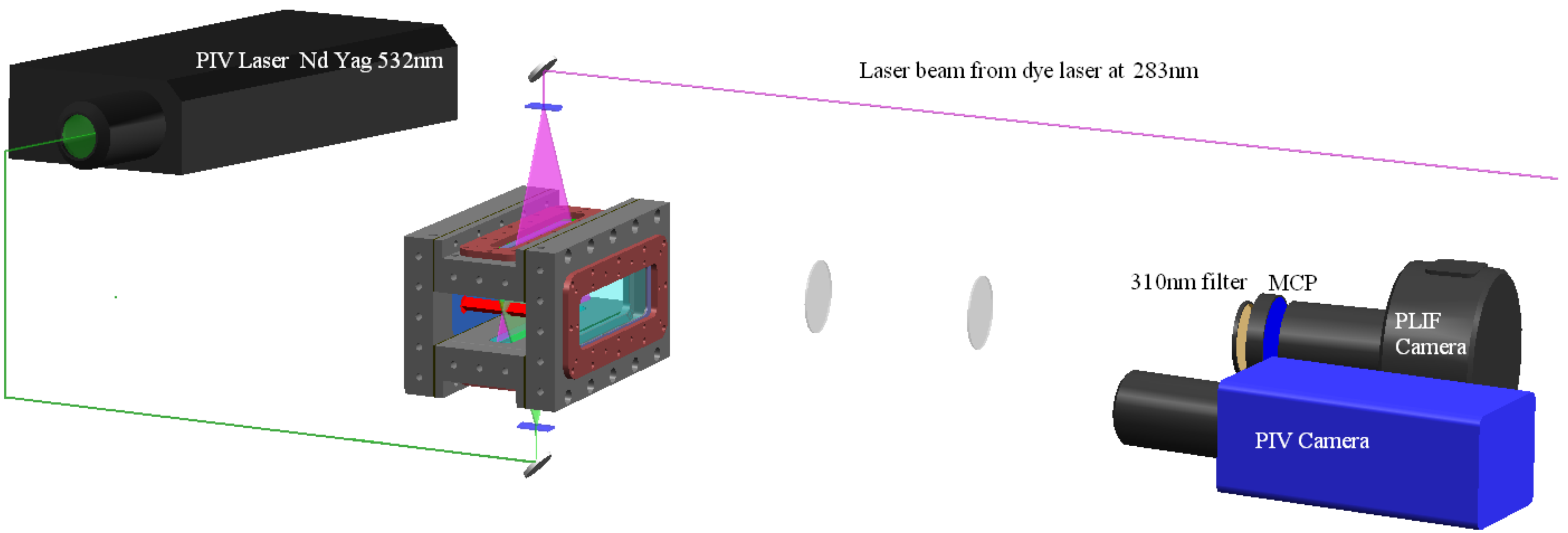

Simultaneous PIV PLIF setup

Stable Flame at $\phi = 0.85$

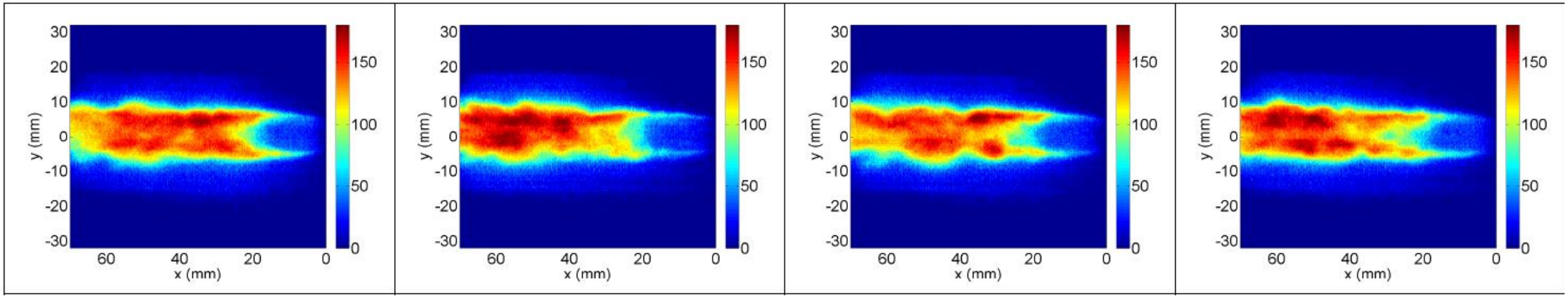

High speed chemiluminescence emission images for a stable flame very far from blowoff for $U_m = 18.3$ m/s at $\phi = 0.85$ at 500 frames per second and 100 μs exposure.

Blowoff and near blowoff dynamics

Blowoff curve

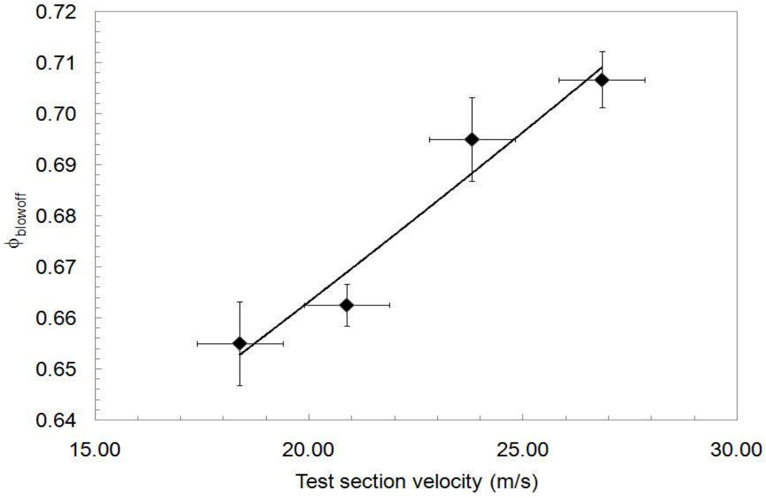

Time history of chemiluminescence near blowoff

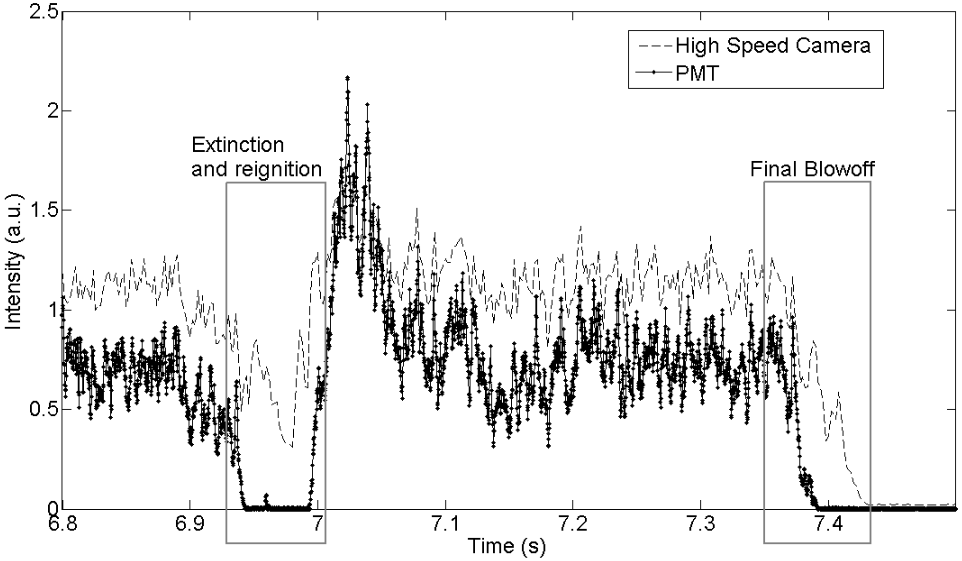

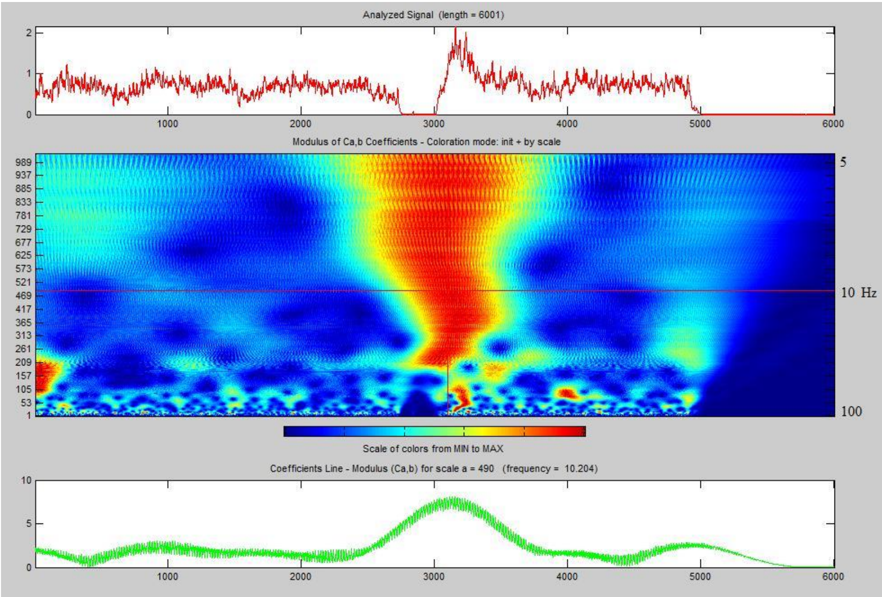

Wavelet Analysis can be a powerful predictive tool for developing an in situ sensor

Extinction reignition and blowoff : movie

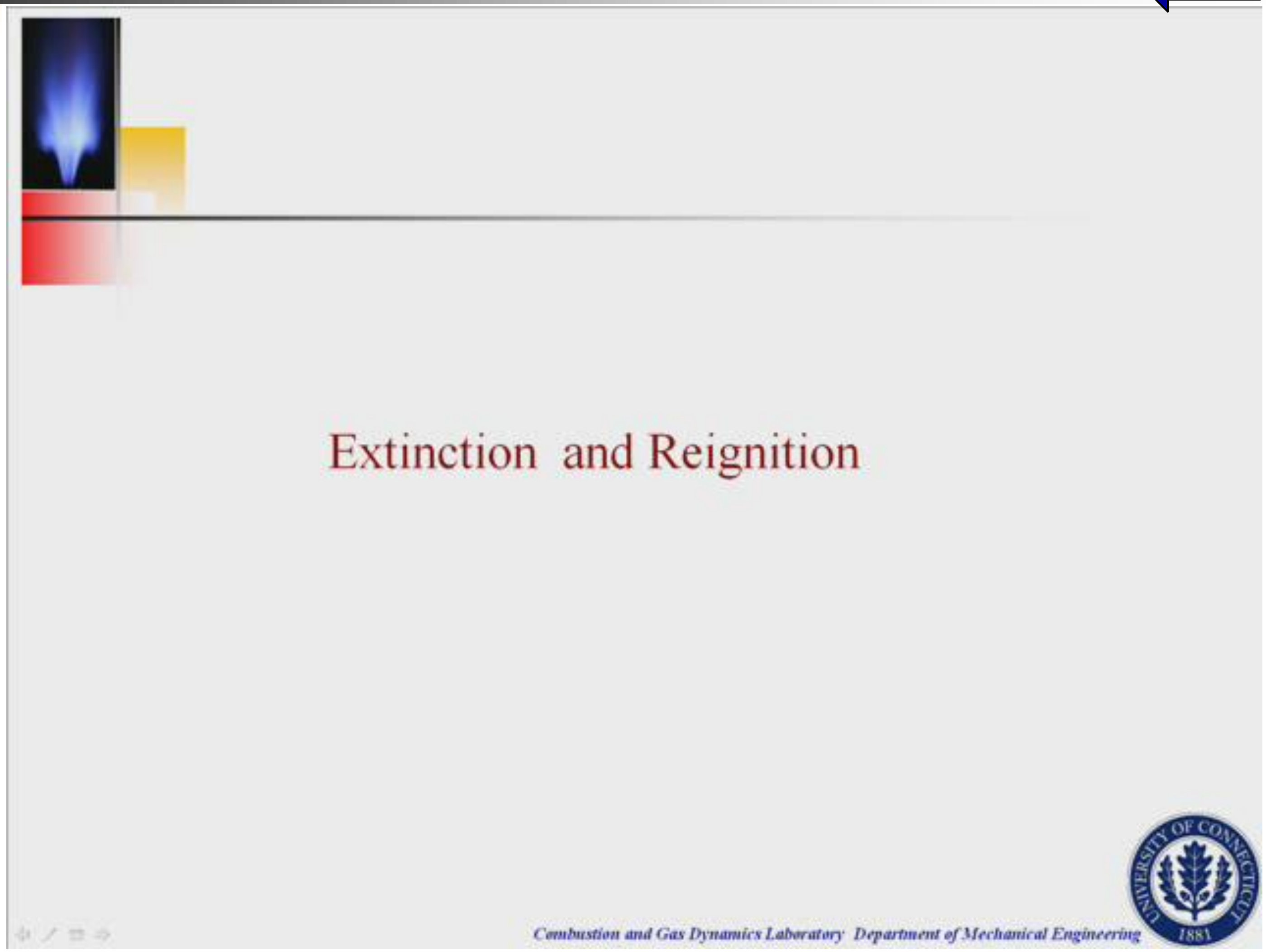

Camera (whole); PMT (wake)

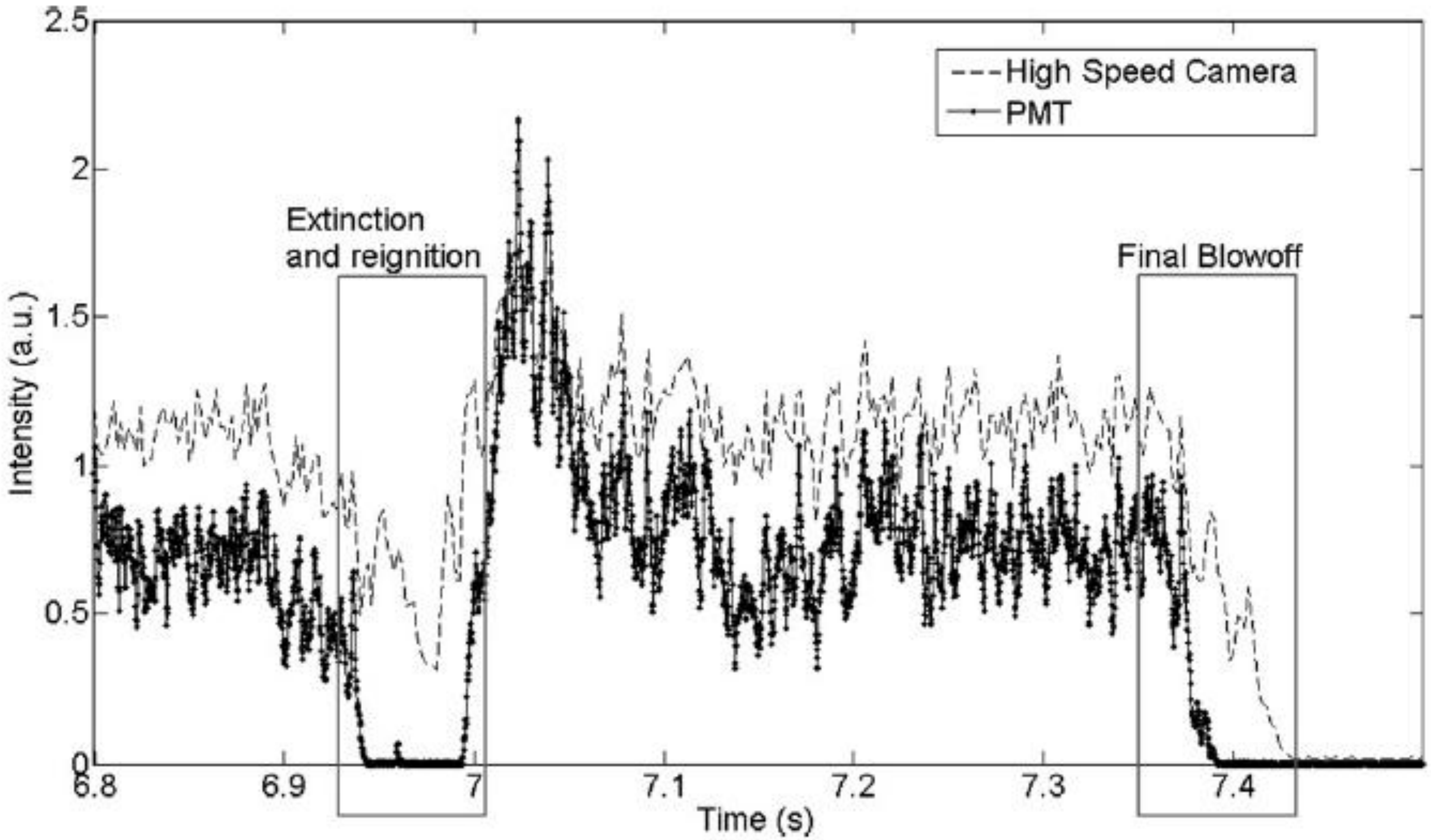

Simultaneous PIV and OH PLIF

Stable flame
$\phi = 0.85$

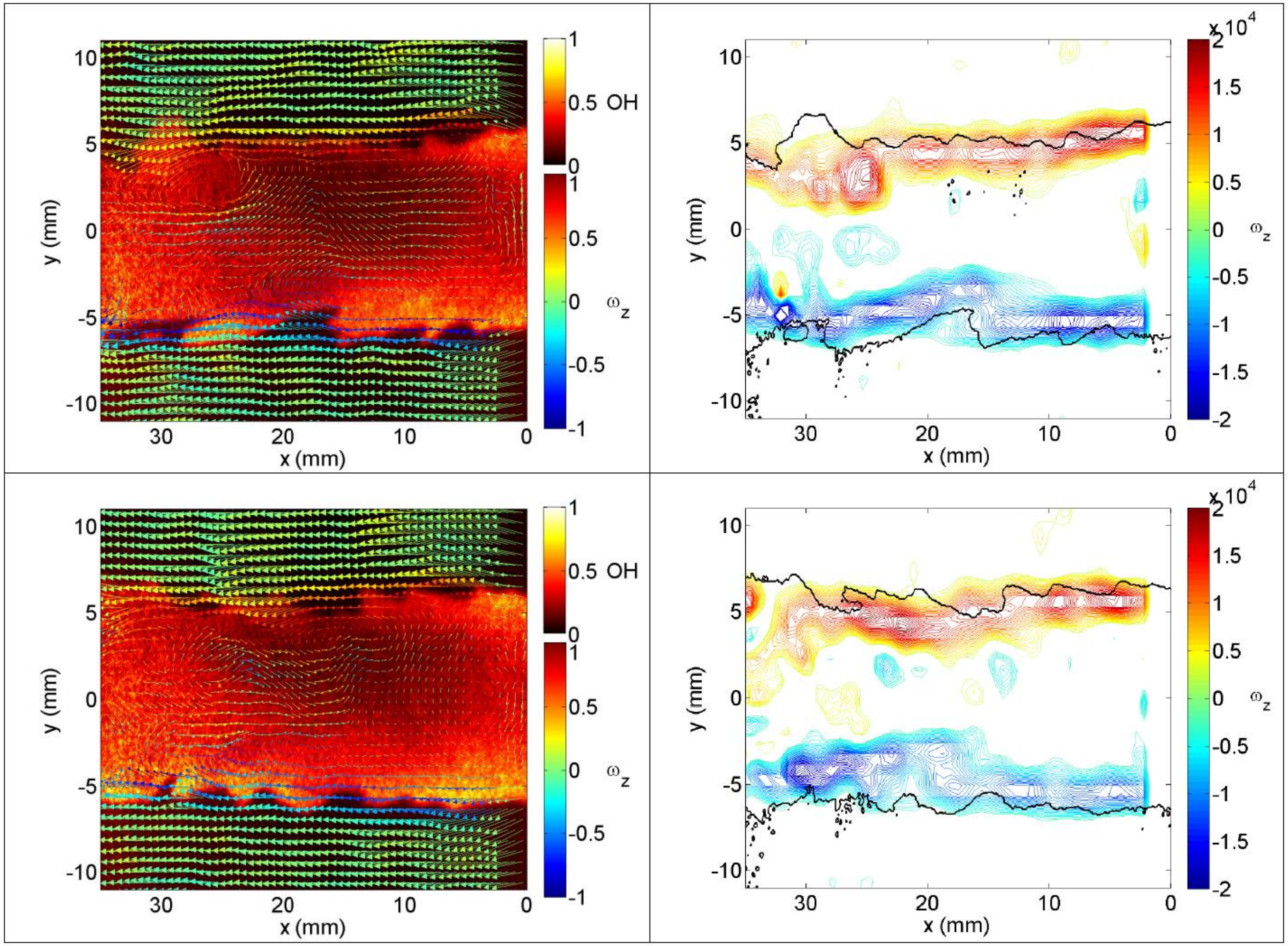

S. Chaudhuri, S. Kostka, S. Tuttle, M. Renfro, B. Cetegen, Combustion and Flame 2011

Extinction along shear layers

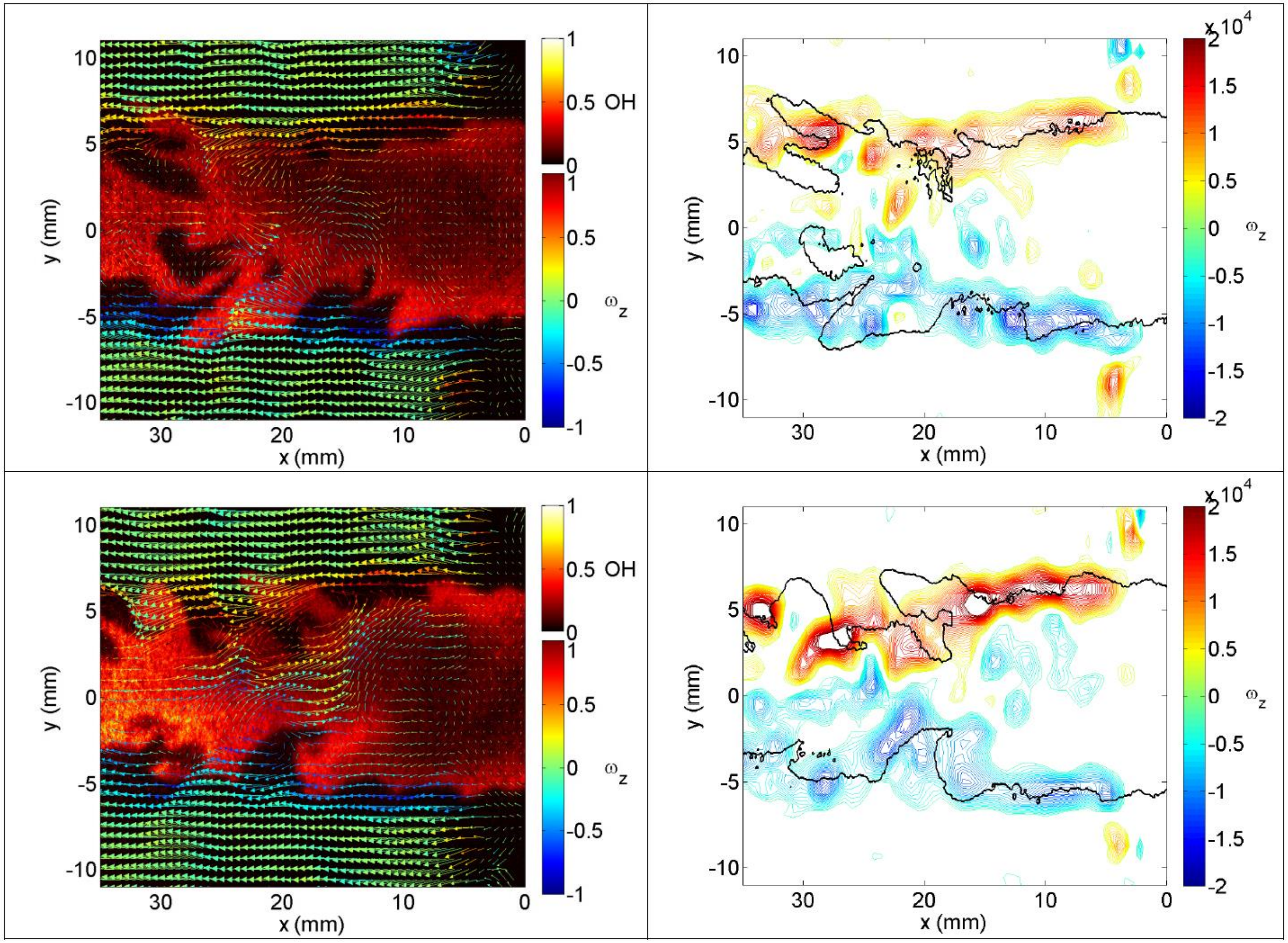

Near blowoff flame
$\phi = 0.65$

Mean profiles of U_x, ω_z and OH

ϕ =0.85

ϕ =0.65

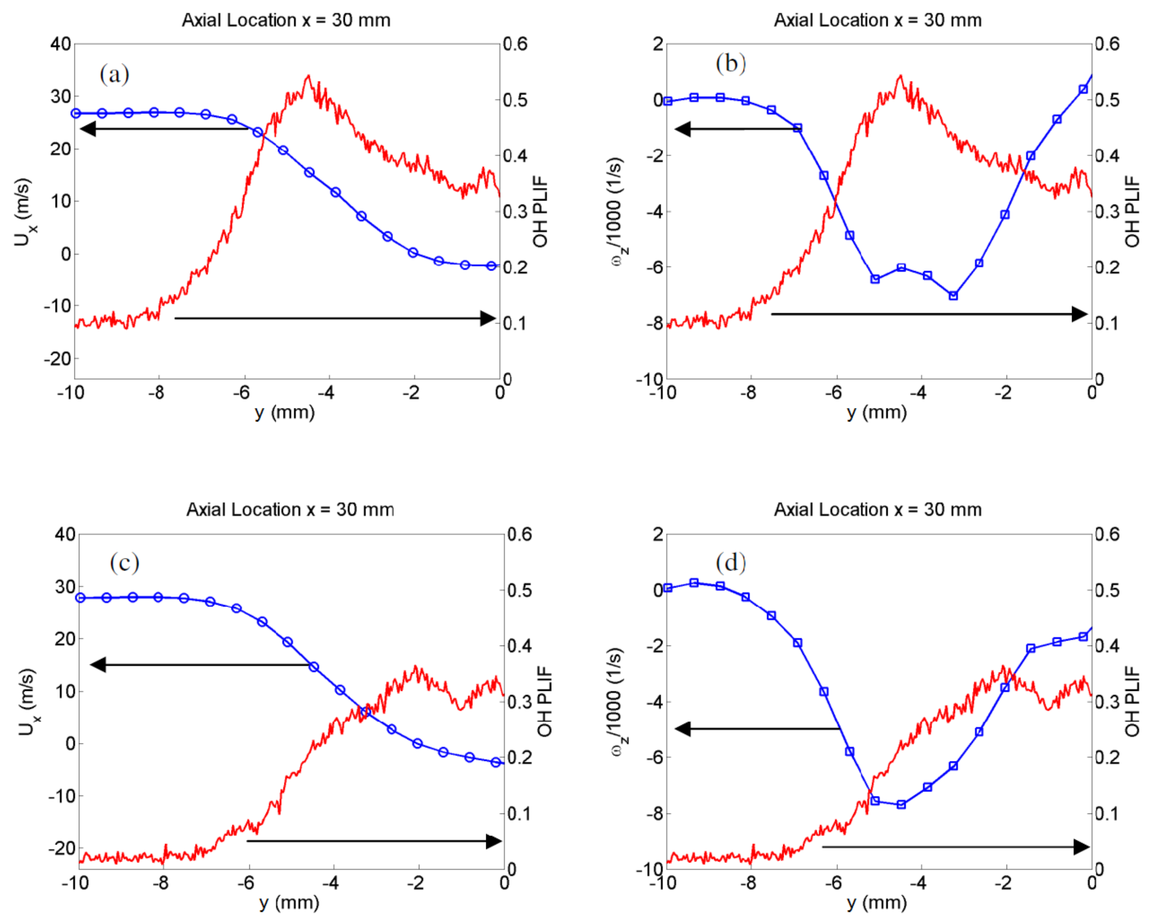

Left panels: Mean axial velocity from PIV superimposed with OH fluorescence signal from PLIF.
Right panels: Mean out of plane vorticity superimposed with OH fluorescence, both at axial locations of 30 mm for ϕ = 0.85 (a,b) and for ϕ = 0.65 (c,d).

Joint probability density functions

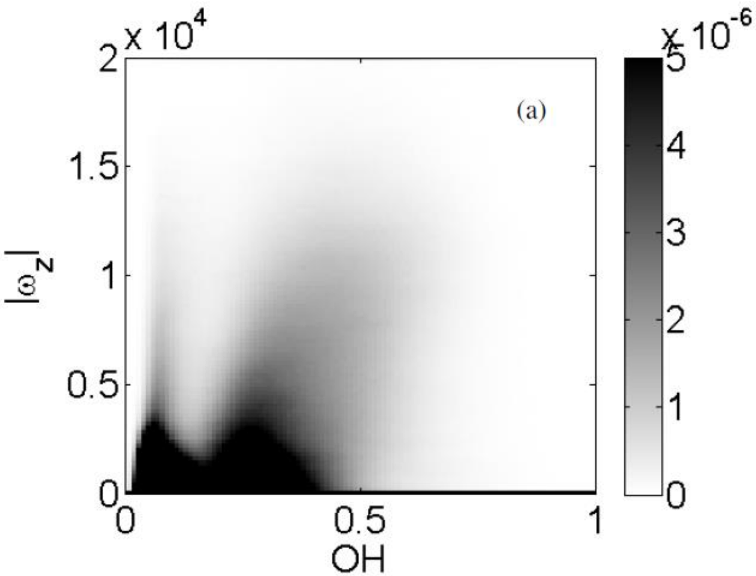

(a) ϕ = 0.85 (far from blowoff)

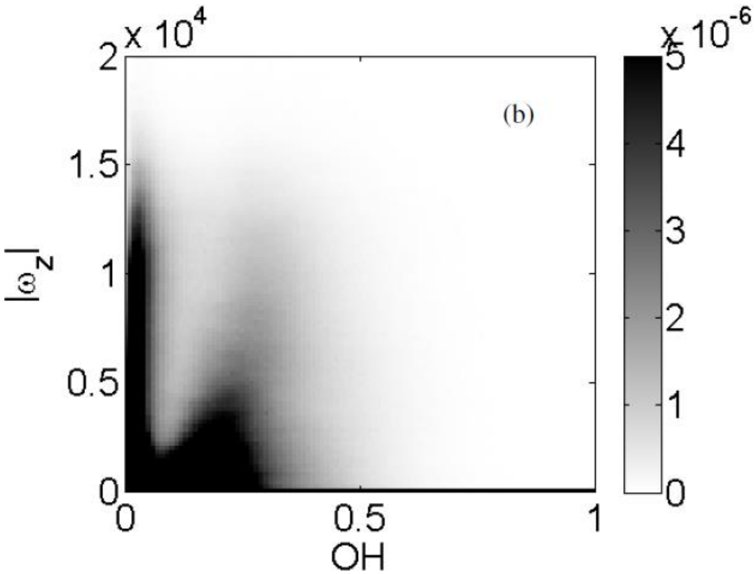

(b) ϕ = 0.65 (near blowoff)

Stretch Rate Pdf

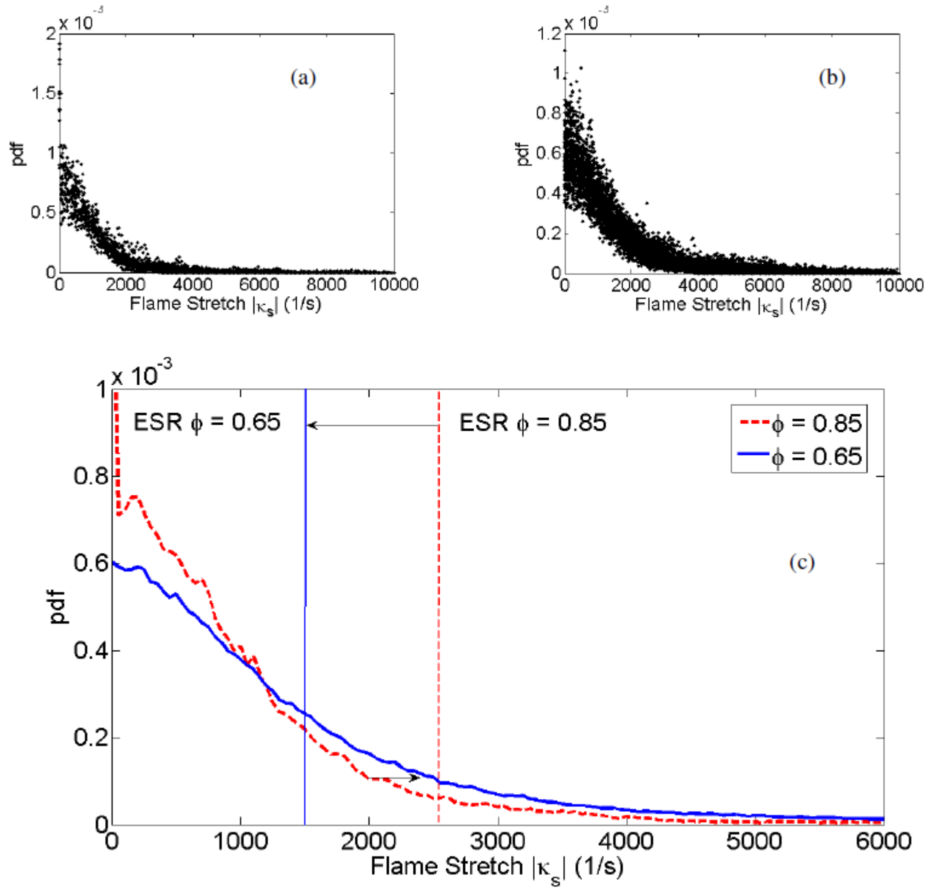

Probability density function of $|K_s|$ at (a) $\phi = 0.85$ (b) $\phi = 0.65$ and (c) Mean pdfs of $|K_s|$ at $\phi = 0.85$ and $\phi = 0.65$.

Extinction along shear layers and recirculation zone burn

Near blowoff flame
$\phi = 0.60$

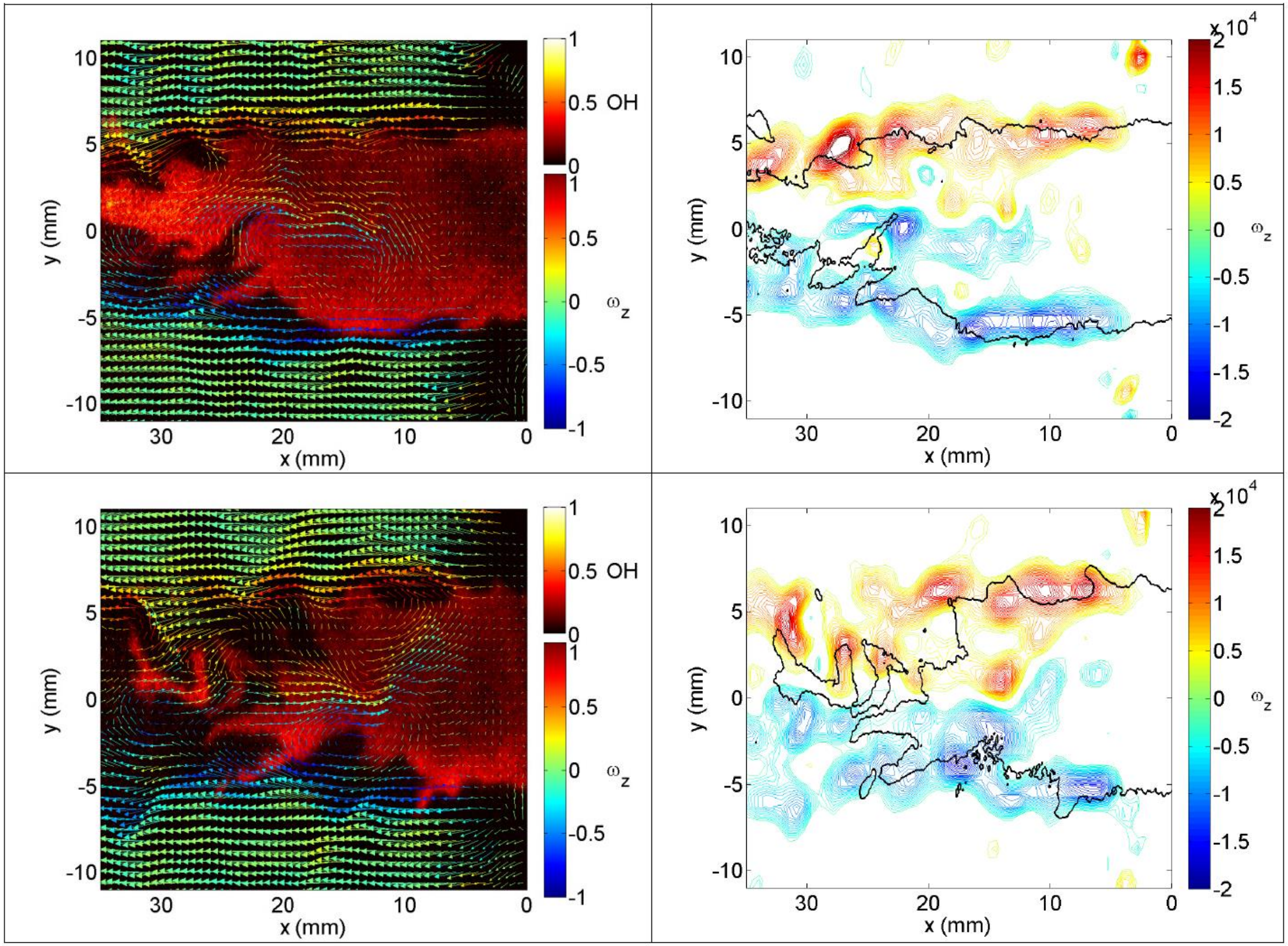

Proposed blowoff mechanism

Towards blowoff $\phi \downarrow$ and hence $S_L \downarrow$, so flame shifts from outside towards the shear layer vortices. Partial flame extinction along shear layers due to $\kappa_{flame} > \kappa_{extinction}$ by convecting vortices.

Non reacting unburnt mixture entrains into RZ and due to favorable flow time scales reacts within RZ . Hence OH and chemiluminescence

Reacting RZ reignites the shear layers to cause reignition

Reacting RZ fails to reignite the shear layers

More parts of the shear layers become "cold" Absolute instability : Asymmetric mode steps in to cause greater perturbations

Blowoff

S. Chaudhuri, S. Kostka, M. Renfro, B. Cetegen, Combustion and Flame 2010

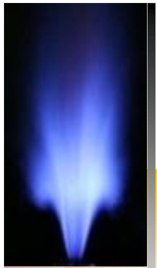

Works at Cambridge: lean CH_4-air flames

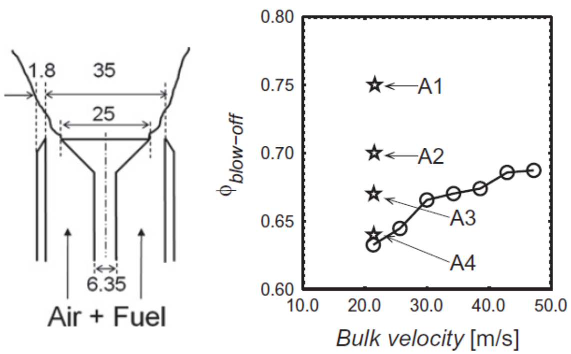

(a) (b)

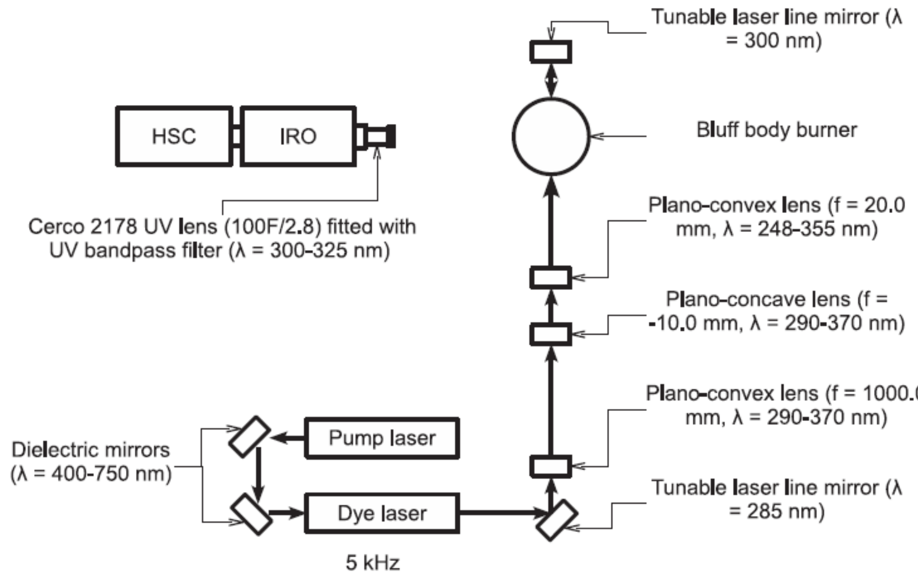

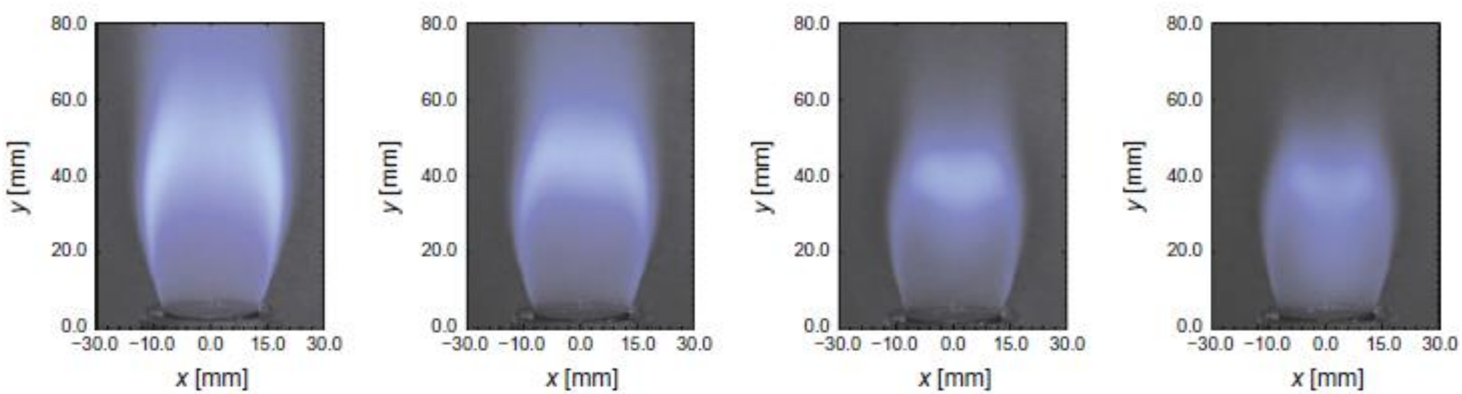

(a) A1 (b) A2 (c) A3 (d) A4

J. Kariuki, J. Dawson and E. Mastorakos, Combustion and Flame 2012

OH PLIF

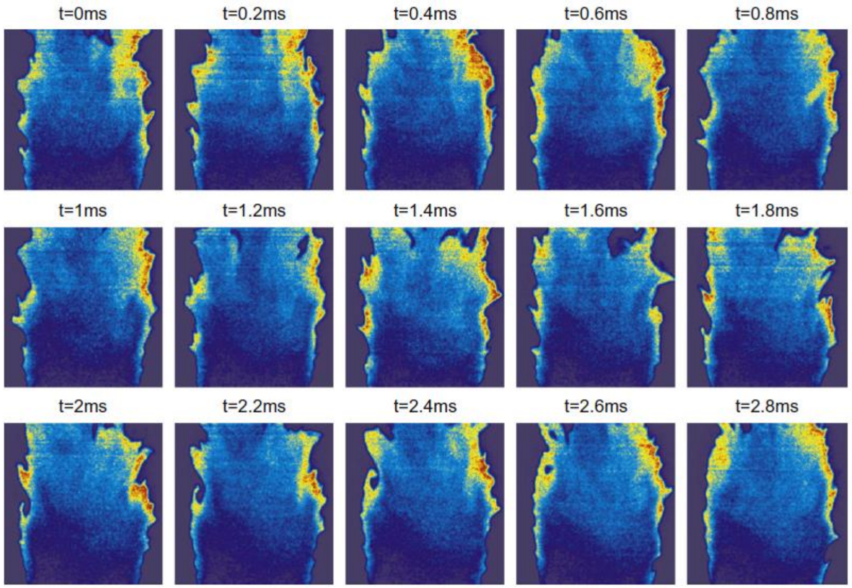

(a)

Far from blowoff

Near blowoff

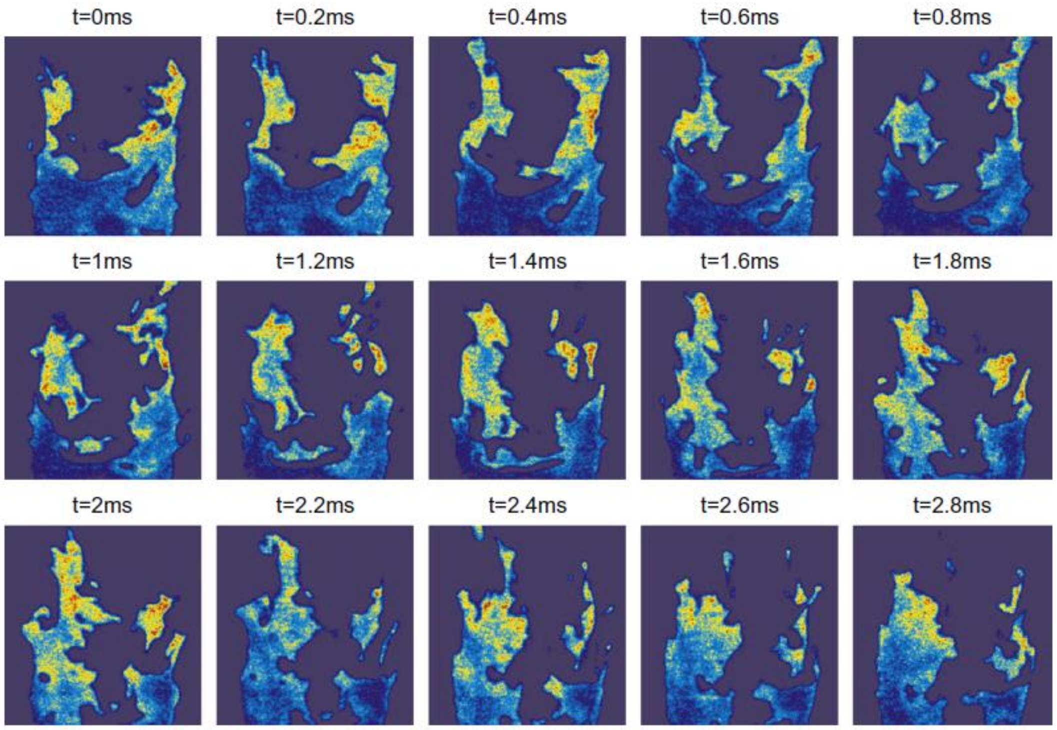

(b)

J. Kariuki, J. Dawson and E. Mastorakos, Combustion and Flame 2012

Blowoff in Vitiated Flows

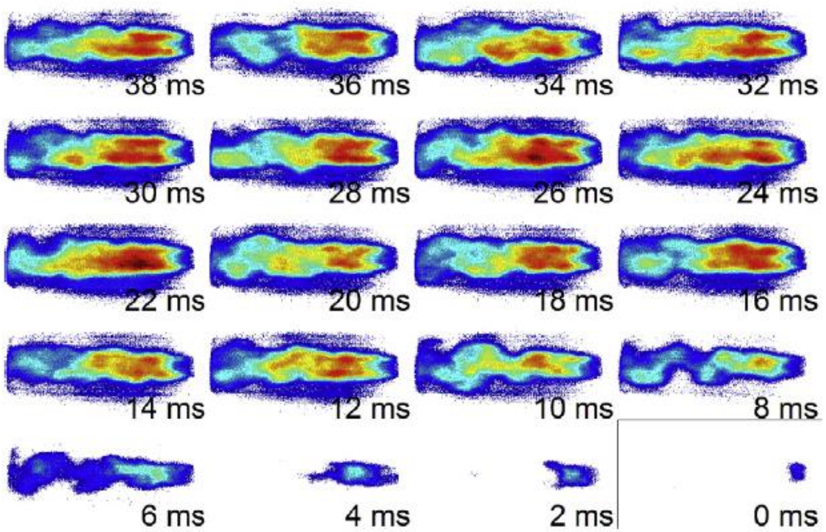

Fig. 9. High-speed chemiluminescence images of a blowoff event at $\phi_T = 0.51$, $\phi_P = 0.15$, and 59 m/s, gathered at 500 frame

Vitiated

Unvitiated

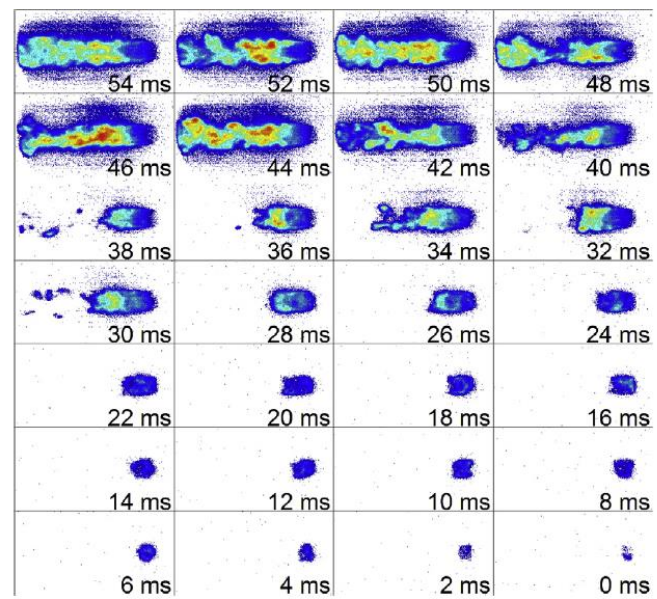

Fig. 10. High-speed chemiluminescence images of a blowoff event at $\phi = 0.65$, $\phi_P = 0.00$, and 18.5 m/s, gathered at 500 frames/s.

S. Tuttle, S. Chaudhuri, S. Kostka, K. Vaughn, T. Jensen, M. Renfro, B. Cetegen, Combustion and Flame 2012

PIV–PLIF of near blowoff vitiated flames

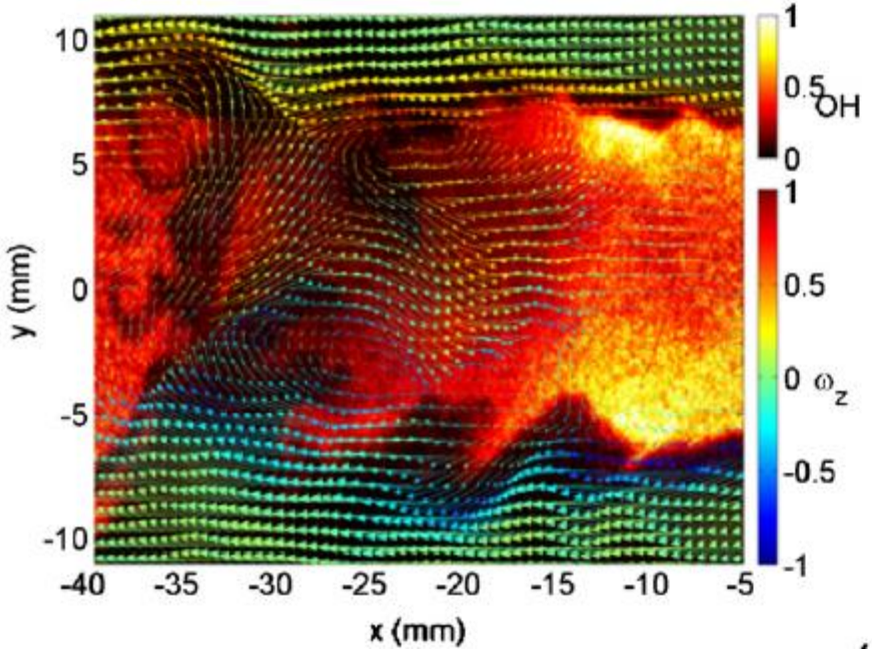

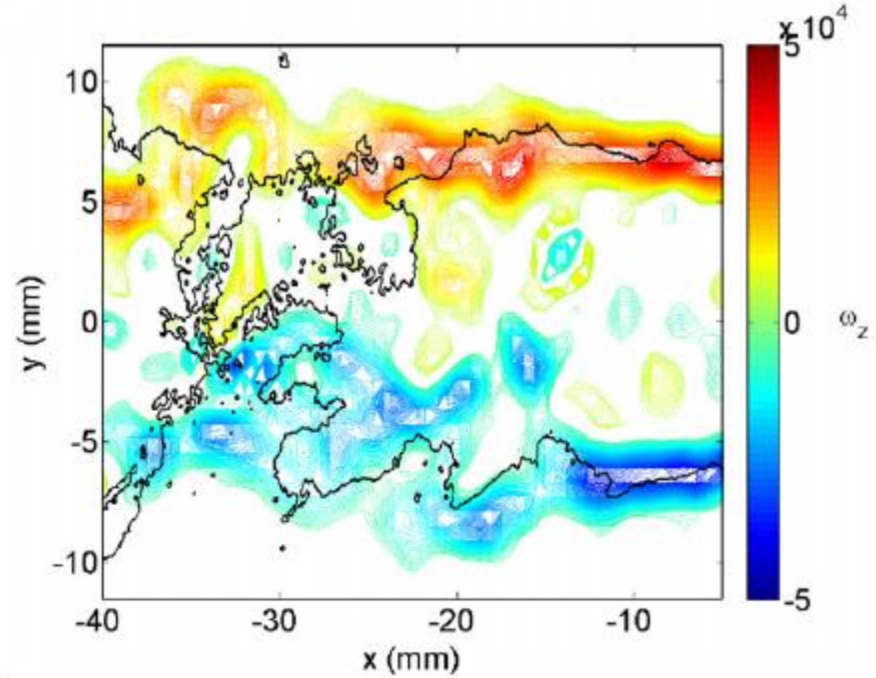

Significant difference between vitiated and unvitiated blowoff

Forced blowoff mechanism

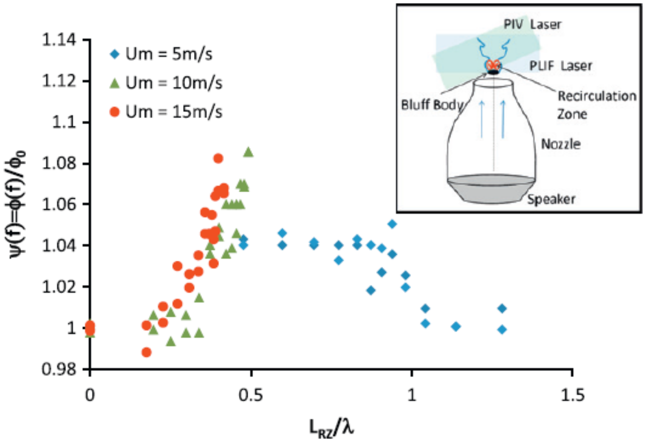

Fig. 1. Ratio of blowoff equivalence ratio at a particular frequency of perturbation with blowoff equivalence ratio at no perturbation as a function of the ratio of L_{RZ}/λ for U_m = 5, 10 and 15 m/s. A schematic of the burner is shown in the inset.

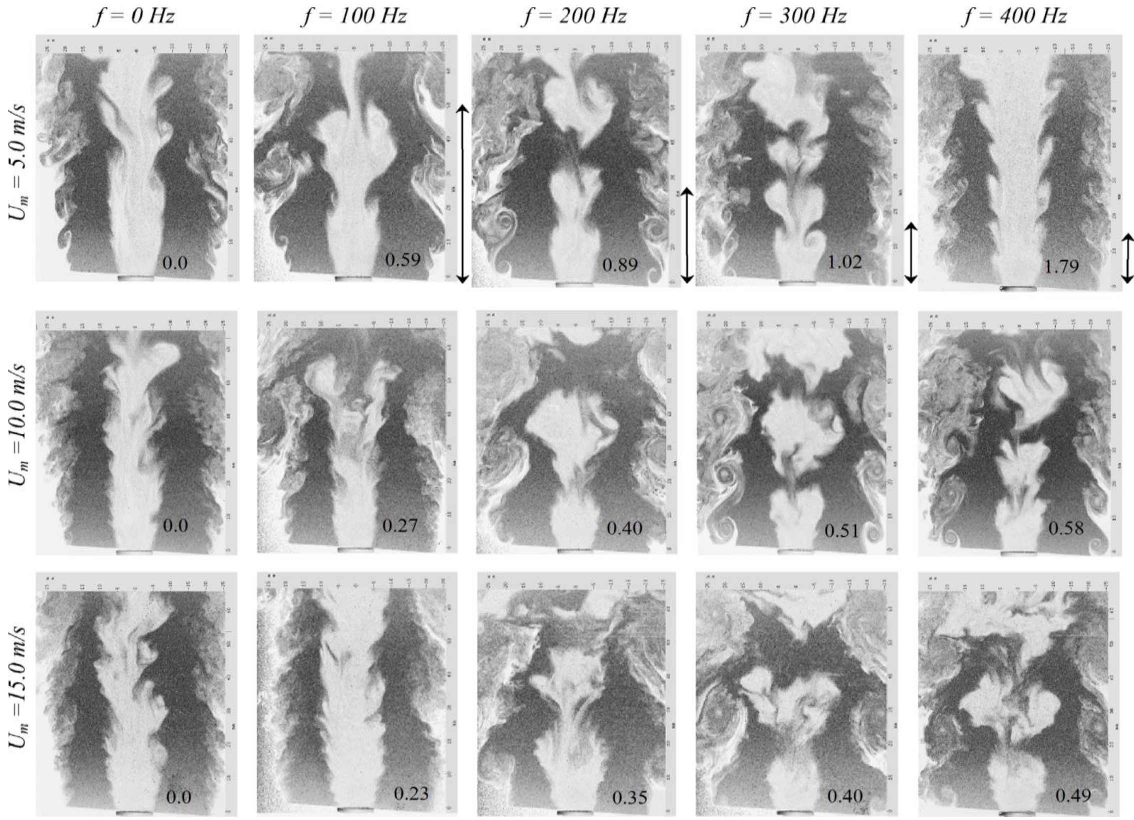

Flame images obtained by reversing the Mie scattering images obtained during the PIV experiments for the 10-mm-diameter disk-shaped bluff-body flame holder (arrows show the length scale $\lambda = U_m/f$). (.The values in black represent the ratio of the length of recirculation zone to λ.

A. Chapparo, B.M. Cetegen, Combustion and Flame 2006

Mean flow and PLIF fields for U_m = 10m/s f = 200Hz $L_{RZmean}/\lambda_{mean}$ = 0.4

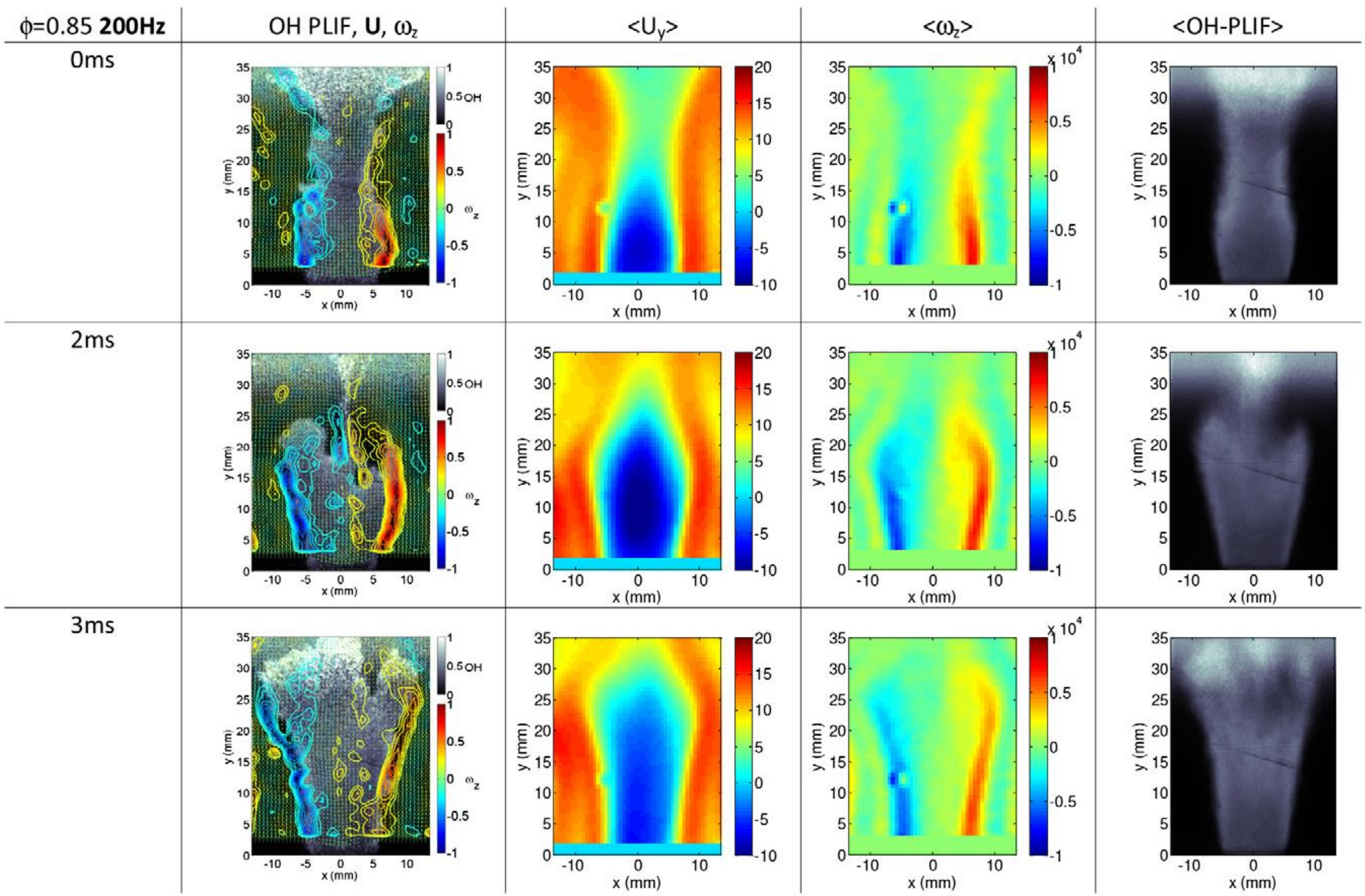

S. Chaudhuri, S. Kostka, M. Renfro, B. Cetegen, Combustion and Flame 2012

Forced Blowoff : Forced Vortex Shedding

Forced Blowoff

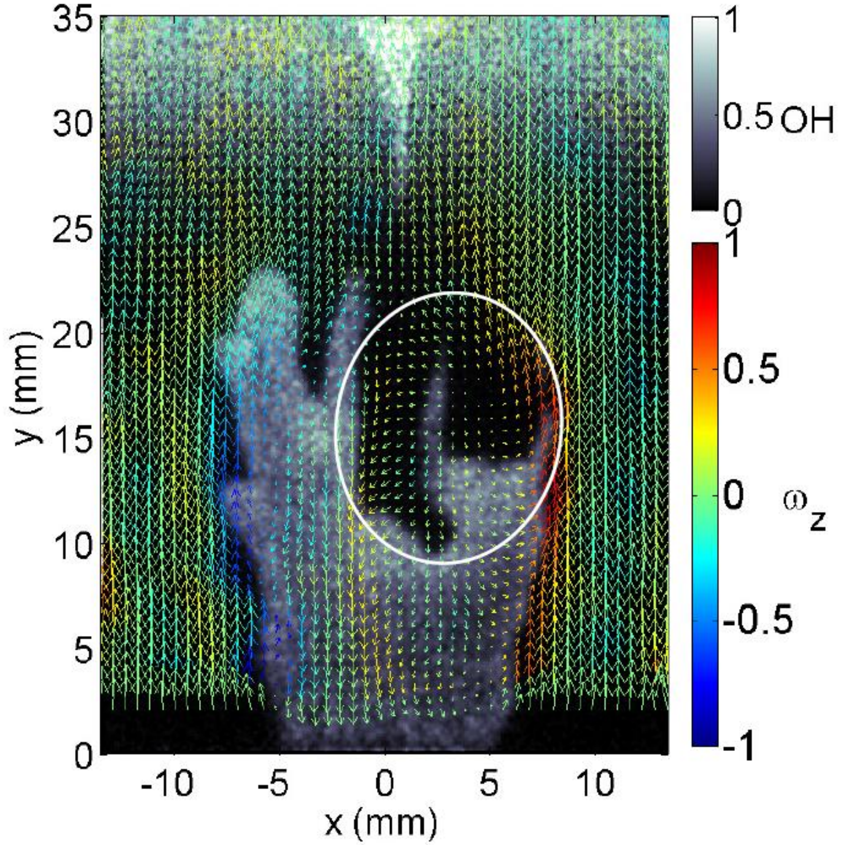

Unforced Blowoff

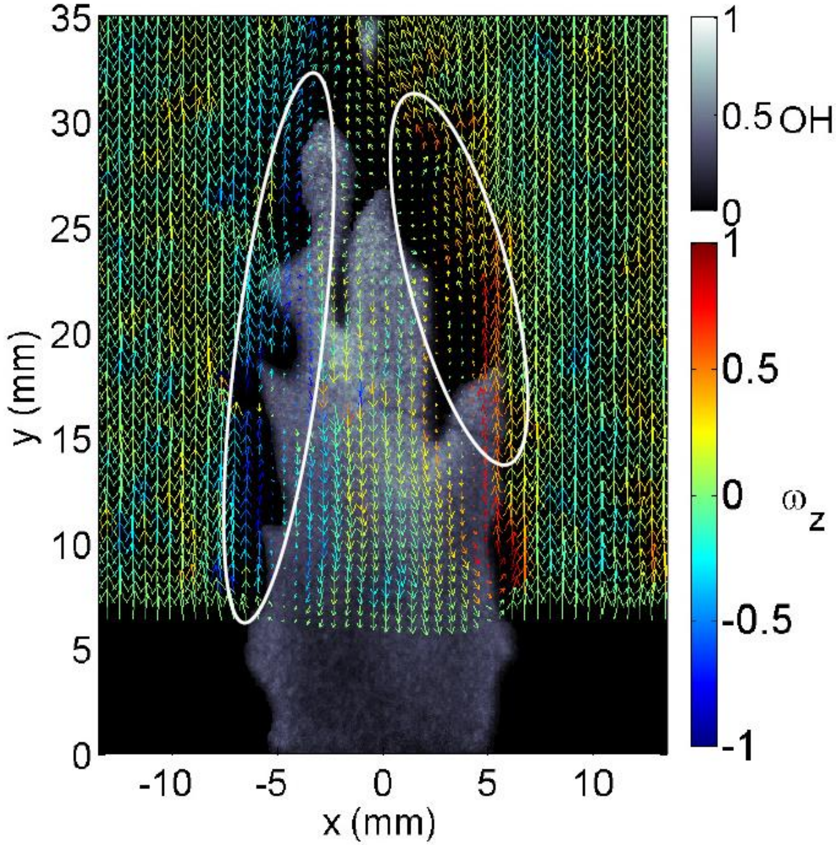

S. Chaudhuri, S. Kostka, M. Renfro, B. Cetegen, Combustion and Flame 2012

Blowoff in Swirl Stabilized Flames (Ga.Tech)

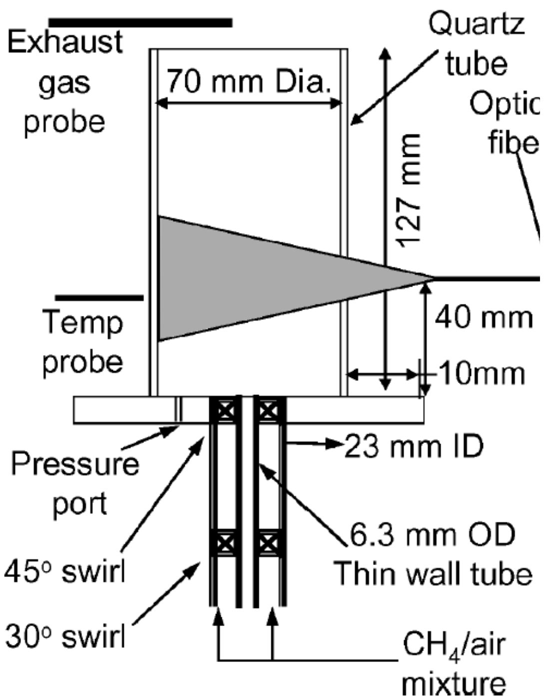

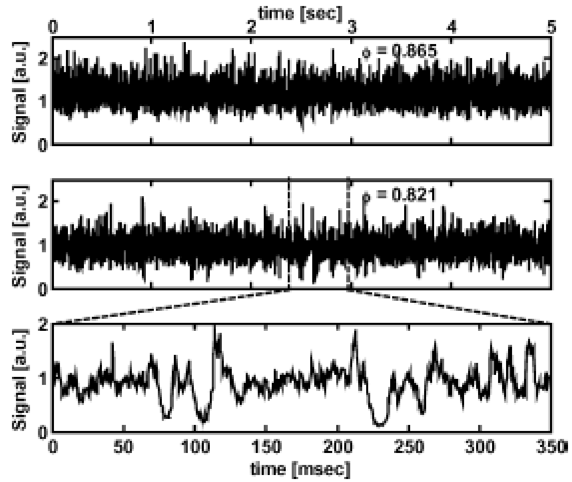

Fig. 2 Time-series data of OH chemiluminescence signal for equivalence ratio $\phi = 0.865$ and 0.821 ($\phi_{LBO} = 0.802$). The expanded time series for the last case is also shown.

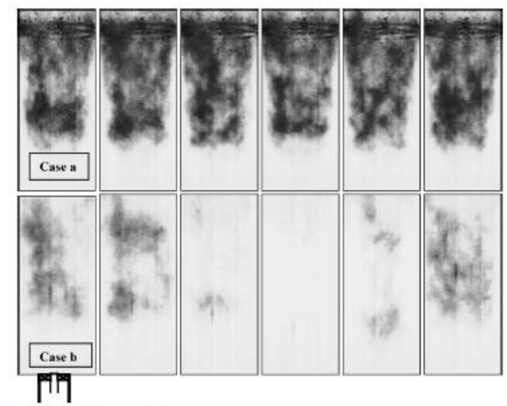

Fig. 3 High-speed visualization images (inverted grayscale): case a, equivalence ratio $\phi = 0.79$, time between images 2 ms; and case b, $\phi = 0.76$, time between images 16 ms showing a nearly total loss of flame followed by reignition ($\phi_{LBO} = 0.745$). The location of the combustor inlet is indicated in the first image of case b.

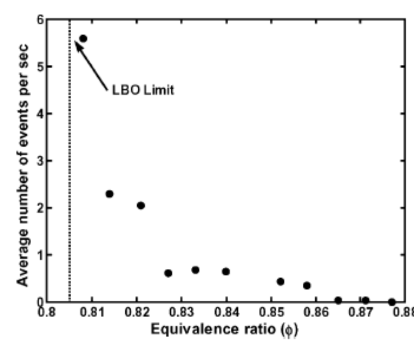

Fig. 5 Variation of average number of events per second as a function of equivalence ratio: · · · ·, LBO limit for these conditions.

T. M. Muruganandam, S. Nair, D. Scarborough, Y. Neumeier, J. Jagoda, T. Lieuwen, J. Seitzman , B. Zinn, Journal of Propulsion and Power, 2005

Blowoff in Swirl Stabilized Flames (DLR)

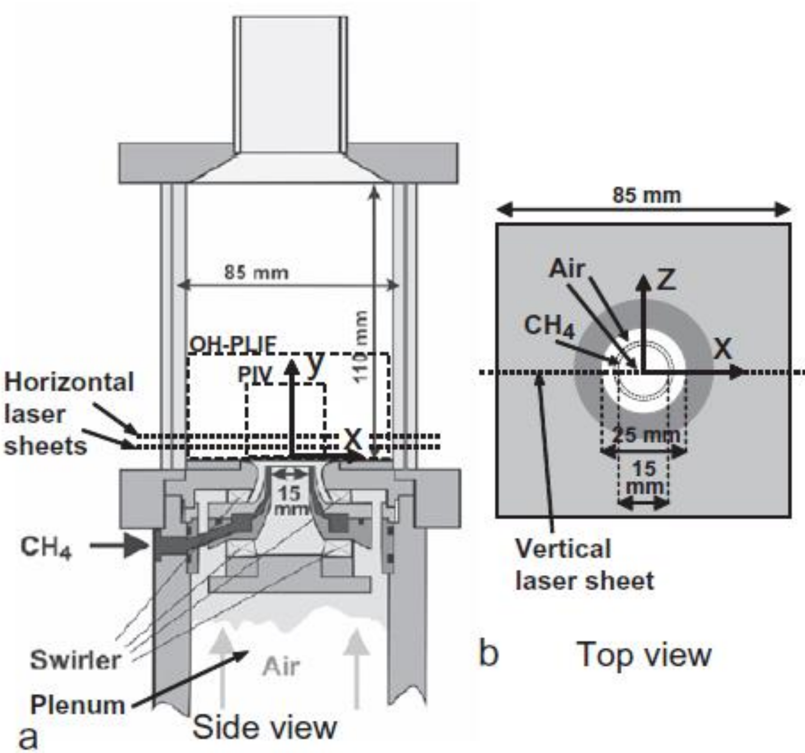

Experimental Setup

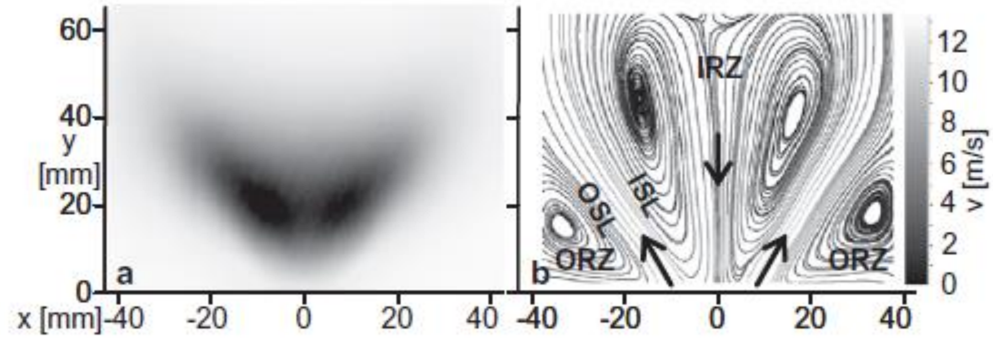

Time averaged OH* and streamlines

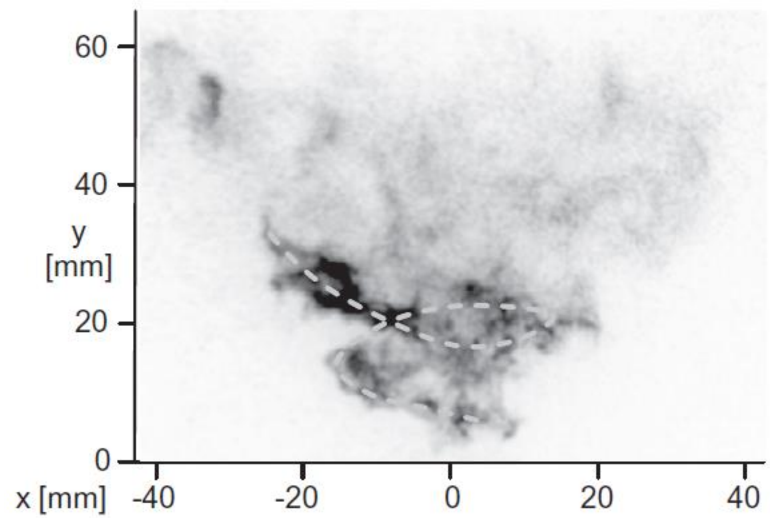

M. Stoehr, I. Box, C. Carter, W. Meier, Proceedings of the Combustion Institute 2011

Near and Final Blowoff

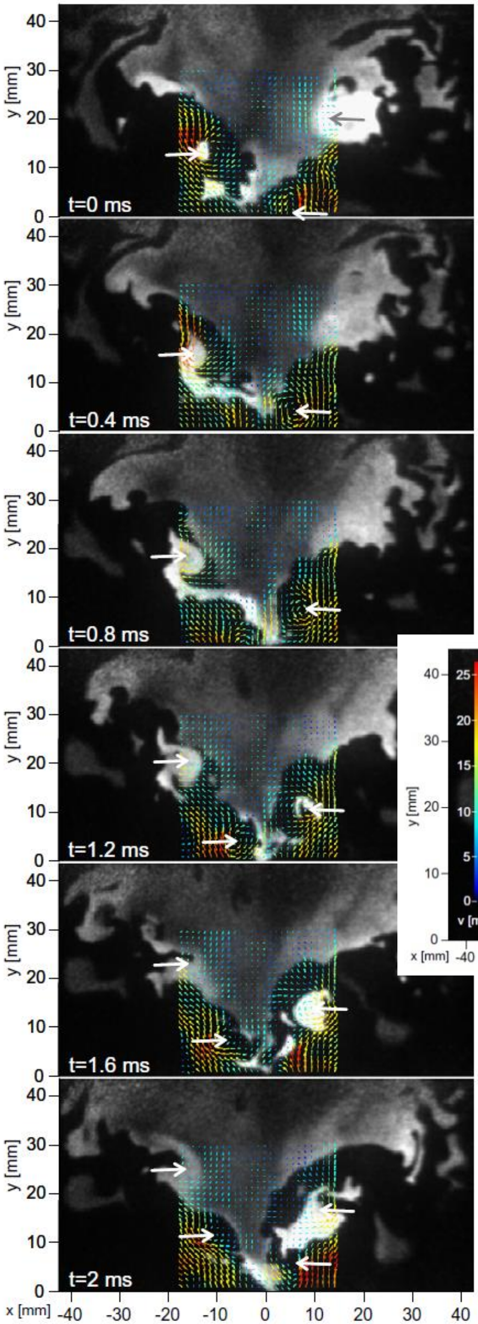

Consecutive images with PIV-PLIF near blowoff

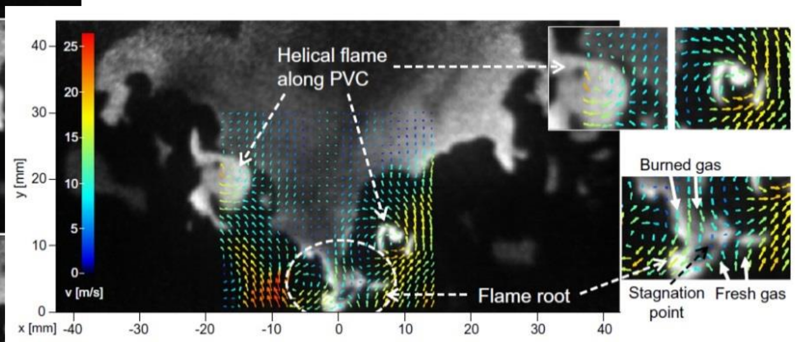

Enlarged views

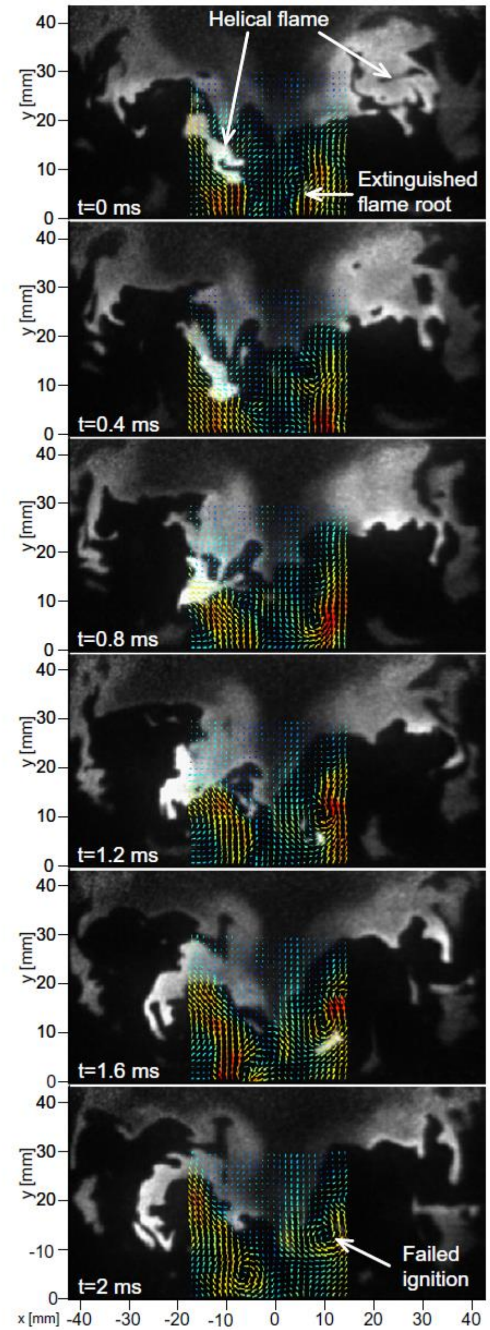

Final blowoff

Swirling flame blowoff

- Reaction occurs in helical zone along PVC (low SR); lower stagnation zone (high SR)
- This lower root flame region determines the rest of the state of the flame (in PVC), is inherently unstable.
- Finding is consistent with earlier work by Muruganandam and Seitzman who controlled blowoff by a pilot flow at the center.
- If the root remains extinguished for more than 2 ms (time scale of PVC) no relight is possible and flame blows off.

M. Stoehr, I. Box, C. Carter, W. Meier, Proceedings of the Combustion Institute 2011

DNS of H_2-air flames

- DNS of temporally evolving planar premixed jet flame [1]
- Lean H2-air (Φ=0.7) jet at Re = 10,000, T_u = 700 K

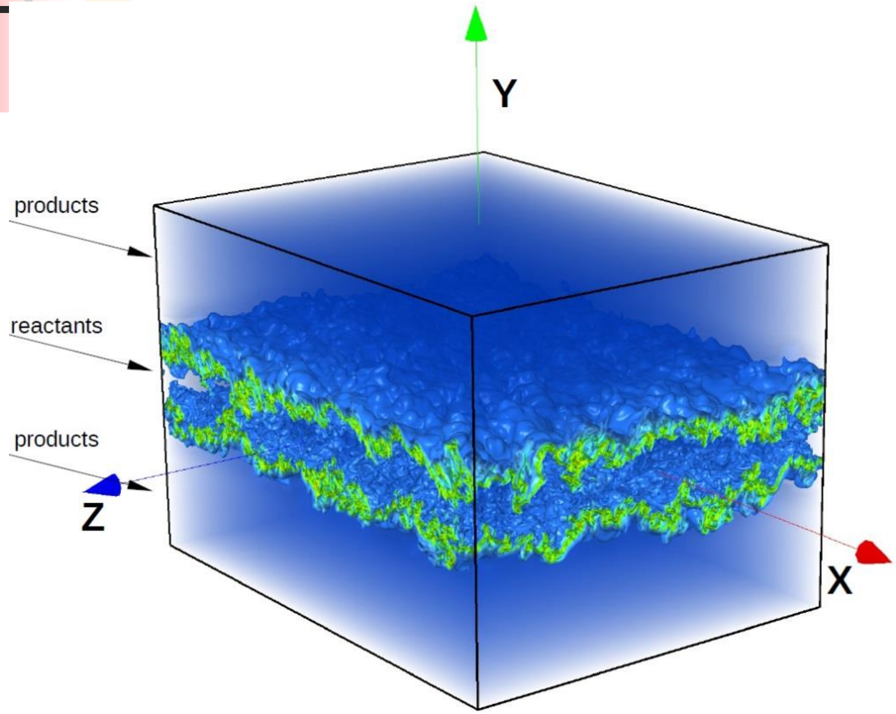

	H (mm)	ΔU (m/s)	Da_{jet}
Da-	2.7	312.6	0.13
Da+	5.4	156.3	0.54

- DNS code S3D [2]; Mechanism of Li *et al.,* [3] (9 species, 19 reactions).
- Simulations performed on 120,000 cores of Jaguar Cray XT5 at ORNL by J. H. Chen group at Sandia.

[1] Hawkes et al. 2009, Comb. Flame. 159-2690.
[2] Chen et al. 2009, Comp. Sci. Disc. 2-015001.
[3] Li et al. 2004, Int. J. Chem. Kin., 80.

Alignment statistics between surface normal and principal component of strain rate tensor

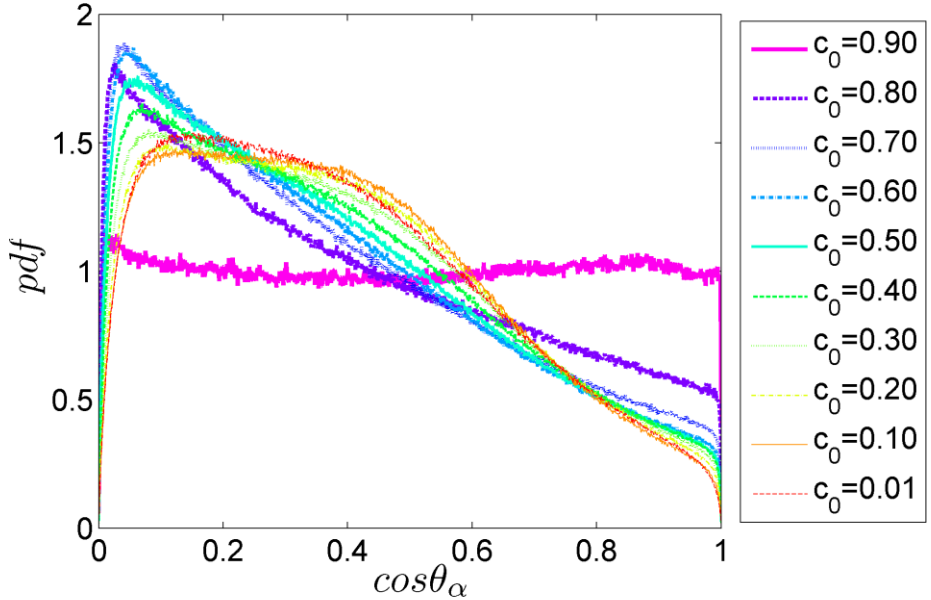

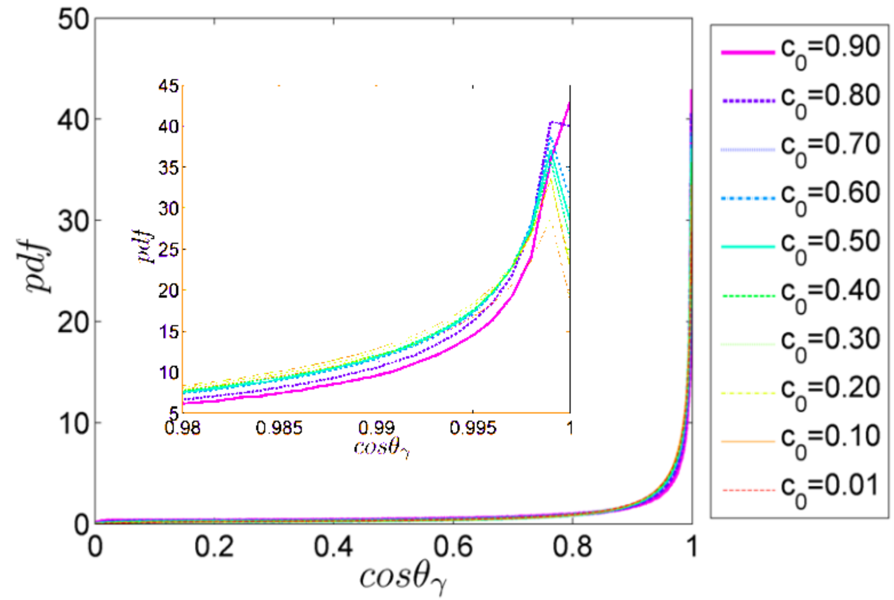

In both cases the flame normal is almost perfectly aligned with the most compressive strain and this alignment improves with increasing c_0

S. Chaudhuri, H. Kolla, E. Hawkes, J. H. Chen, C.K. Law under review JFM

Thanks and Questions